

Forecasting CPI inflation under economic policy and geo-political uncertainties

Shovon Sengupta
Fidelity Investments
BITS Pilani, Hyderabad
ssg.plabon@gmail.com

Tanujit Chakraborty*
Sorbonne Center for AI
Sorbonne University
tanujit.chakraborty@sorbonne.ae

Sunny Kumar Singh
BITS Pilani, Hyderabad
sunny.singh@hyderabad.bits-pilani.ac.in

Abstract

Forecasting a key macroeconomic variable, consumer price index (CPI) inflation, for BRIC countries using economic policy uncertainty and geopolitical risk is a difficult proposition for policymakers at the central banks. This study proposes a novel filtered ensemble wavelet neural network (FEWNet) that can produce reliable long-term forecasts for CPI inflation. The proposal applies a maximum overlapping discrete wavelet transform to the CPI inflation series to obtain high-frequency and low-frequency signals. All the wavelet-transformed series and filtered exogenous variables are fed into downstream autoregressive neural networks to make the final ensemble forecast. Theoretically, we show that FEWNet reduces the empirical risk compared to single, fully connected neural networks. We also demonstrate that the rolling-window real-time forecasts obtained from the proposed algorithm are significantly more accurate than benchmark forecasting methods. Additionally, we use conformal prediction intervals to quantify the uncertainty associated with the forecasts generated by the proposed approach. The excellent performance of FEWNet can be attributed to its capacity to effectively capture non-linearities and long-range dependencies in the data through its adaptable architecture.

1 Introduction

The monetary policy framework at central banks relies heavily on forecasts of various macroeconomic variables. Forecasts have also grown in importance as a means of communication for central banks during the past 20 years, and they have the potential to shape public and market expectations. Numerous studies have examined central bank forecasting from various angles due to the paramount significance of these predictions [1–5]. Forecasting, particularly in the context of different macroeconomic policy variables, is one of the major focus areas in this domain. Inflation is one such policy variable considered instrumental in designing an economy’s overall monetary policy. Thus, a deeper understanding of the factors that help forecast inflation accurately is fundamental to policymakers at the central bank [1]. Over the past few decades, emerging market economies such as Brazil, Russia, India, and China (BRIC) have undergone significant changes in their macroeconomic conditions, including shifts in monetary policy frameworks such as inflation targeting, increased globalization, and the impact of events like the financial crisis and the recent pandemic. These shifts make predicting key macroeconomic variables like consumer price index (CPI) inflation quite challenging [2]. Given these dynamic changes in the macroeconomic environment, factors like economic policy uncertainty and geopolitical risk might offer critical insights to forecast inflation accurately.

Due to the significance of inflation forecasting exercise for monetary policy, central banks often depend on distinct models, namely structural and non-structural. The structural models, which are different versions of Phillips curve models, are derived from economic theory. On the other hand, the non-structural models, such as linear univariate and multivariate time-series models, aim to utilize the unique characteristics of the data without explicitly depending on any economic theory [3]. Non-structural models often prioritize forecast

*Corresponding Author

accuracy above causal inference and are particularly valuable for short-term, out-of-sample forecasting. Linear time series models such as autoregressive integrated moving average (ARIMA) and vector autoregressive (VAR) are limited in their ability to account for business cycles, periods of extreme volatility caused by macroeconomic uncertainties, and structural changes. As a result, non-linear, hybrid, and machine learning models have become increasingly popular to address these shortcomings. Furthermore, the existing linear time series forecasting methods bring several undesirable properties, ranging from high sensitivity to model specification to high-frequency data requirements [4]. This is especially important for forecasting inflation or similar macroeconomic variables that are only available at the monthly, quarterly, and annual frequency. This issue is more serious for emerging market economies where the quality of macroeconomic data is not up to the mark. Given such issues related to inflation data in emerging countries, machine learning (ML) models and combined approaches provide an opportunity to improve forecast performance.

Recently, an increasing number of studies have been conducted on applying ML models for inflation forecasting, both for advanced and emerging market economies. A study conducted in the United States utilized a basic feed-forward neural network to forecast quarterly CPI inflation. The study concluded that this approach was successful in predicting CPI inflation [5]. Neural networks proved more effective than traditional models in predicting the monthly inflation rate for the OECD countries [6]. Their research revealed that neural network models outperformed simple AR models in 45% of the nations, on average, whereas simple AR models performed better in 23% of the countries. Recurrent neural networks, in their various forms, have been discovered to be beneficial for predicting inflation in developed countries [7–10]. In addition, a recent study compared various machine learning models, including lasso regression, random forests, and deep neural networks, to analyze inflation in the United States. The study also considered several external factors, such as cash and credit availability, online prices, housing prices, consumer data, exchange rates, and interest rates [11]. Their research has shown that machine learning models with many covariates consistently outperformed conventional techniques. This superiority can be attributed to nonlinear relationships between historical macroeconomic variables and inflation. This has dispelled doubts about using machine learning and contemporary deep learning architectures in analyzing big data in economics [12]. For emerging market economies, the study of inflation forecasting using advanced ML models is in a nascent stage. Applications of neural networks are evident in developing countries like India, Brazil [13], Russia [14], Turkey, South Africa [15], and China [16]. However, none of the above studies, to the best of our knowledge, have considered exogenous factors like macroeconomic uncertainties for inflation forecasting, especially for emerging markets.

Following events such as the global financial crisis, it has been observed that many countries worldwide have encountered heightened uncertainty. This has had an impact on the decision-making process of individuals and consequently on the overall macroeconomy [17–19]. Although previous studies have primarily examined the connection between uncertainty and the overall economy, the evaluation of the changing relationship between measures of uncertainty and inflation is still in its early stages. It has not yet yielded a definitive conclusion [20, 21]. Gaining insight into the intricacies of inflation dynamics and uncertainty metrics is quite critical for policymakers. Multiple recent studies indicate that both economic policy uncertainty and geopolitical risk significantly influence the movement of inflation within a given sample [20, 22–26]. Consequently, inflation forecasting models that do not incorporate these uncertainties are deemed to be incorrectly specified. The study conducted by [23] examines the effectiveness of different uncertainty measures in predicting inflation. In particular, they use US inflation data and the economic policy uncertainty index (EPU) to compare how well the vector autoregressive fractionally integrated moving average (VARFIMA) model performs at making predictions compared to other models. The study conducted by [27] examined the predictive impact of Economic Policy Uncertainty (EPU) on stock market volatility in the United States and the United Kingdom. The findings suggest that EPU has a significant positive effect on volatility. However, this positive relationship weakens when the signal quality is low. [28] asserted that Economic Policy Uncertainty (EPU) has a crucial impact on enhancing the predictive accuracy of models forecasting stock market volatility. The study conducted by [29] investigated the impact of policy uncertainty in the United States and Europe on the short-term pricing model for gold. The study conducted by [30] investigated the impact of Economic Policy Uncertainty (EPU) on predicting future real economic activities in the UK and European economies. For an extensive analysis and thorough examination of different methods for quantifying uncertainty, as well as the impact of economic policy uncertainty on various economic activities such as stock market returns, corporate capital investments and spending, corporate finance, and risk management, please refer to the publication by [31]. On the other hand, the effect of geopolitical risk uncertainty (GPRC) has been studied extensively by [24]. A recent study by [32] aims to link geopolitical risk with the reduction of firm values as well. The studies covering the impact of various uncertainty measures on different economic activities are still in the nascent phase, and this study in turn, presents a way to accommodate the roles of EPU and GPRC in forecasting inflation numbers.

Wavelet analysis has shown remarkable promise in analyzing financial time series, due to its ability to

distillate crucial information from the financial data. It is their structural flexibility that allows them to handle irregular time series data more effectively for long-term time series forecasting [33]. Its ability to spot the time regime shifts and breakpoints allows it to discover important signals within the time series data. Broadly, wavelets are functions that can decompose the original time series into two sub-components: one concerning the low-frequency or deterministic component and the other concerning the high-frequency or stochastic component of the series. This process aims to reduce the effect of ‘noise’ in the forecast and is found to be quite useful in dealing with a variety of non-stationary signals, a common feature of financial and macroeconomic time series data, as they are constructed over finite time intervals and can represent the ‘local’ elements in both time and scale [34]. Several applications of wavelet analysis can be found in forecasting exchange rates, GDP growth, crude oil prices, stock market prices, Taiwan stock index, S&P dividend yield, trade prices, expenditure and income, price movements, money growth, and inflation [35, 36], volatility in foreign exchange markets, car sales from the last decades [37]. A wide variety of hybrid models combining wavelets and neural networks have been studied for forecasting natural gas prices [38], future trading [39], short-term electricity load [40, 41], energy price forecasting [42], oil prices [35], stock index [43]. Apart from forecasting, the application of wavelet analysis can be found in various areas of finance: [44] analyzed the association between stock price and inflation rate using wavelet analysis, [45] explored the aspect of assessment of the risk in the emerging markets, [46] studied the value at risk in the metal markets. [47] examined the impact of the global financial crisis on the multi-horizon nature of systematic risk and market risk using a wavelet multi-scale approach. [48] used wavelet neural networks for the prediction of corporate financial distress. However, none of the above studies have utilized inflation series and its causal counterparts for long-term forecasting.

Against this background, the primary aim of this study is to create a filtered ensemble wavelet neural network (FEWNet) model. This model belongs to a novel category of machine learning models that combine traditional neural networks with wavelet models. The objective is to generate accurate long-term forecasts for CPI inflation in BRIC countries while taking into account economic and geo-political uncertainties. FEWNet can produce reliable long-term forecasts for CPI inflation of BRIC countries conditioned on economic and geopolitical uncertainties. In analyzing macroeconomic policy variables like CPI inflation, the wavelet decomposition can extract the low-frequency components of the series without sacrificing the fundamental characteristics of the original time series. This model also integrates a layer for feature engineering aspects by extracting the trend components using the Hodrick-Prescott (HP) filter and cyclical elements using the Christiano-Fitzgerald (CF) ideal band-pass filter in the forecasting exercise. Initially, the observed time series (CPI inflation) and exogenous factors (EPU and GPRC) undergo decomposition into their trend and cyclical components using HP and CF filters in the first phase. Subsequently, in the second phase, all the trend and cyclical components are modeled as auxiliary inputs within the FEWNet framework, along with the wavelet-transformed details and smooth coefficients of the CPI inflation. This comprehensive approach aims to generate forecasts for 12 months and 24 months ahead. Conditioning inflation forecasts on policy uncertainty and risk uncertainty would capture the inflation or deflation effects of uncertainty. We argue using wavelet coherence analysis that there exists a relationship between EPU and GPRC with that of CPI inflation for BRIC economies. We show that the data-generating properties of inflation (persistence and volatility) are associated with the movements in EPU and GPRC. Proposed FEWNet generates out-of-sample forecasts in a recursive manner, and using several statistical metrics and tests, we compare its performance with alternative forecasting methods. Theoretical results on empirical risk minimization are also presented for the FEWNet. Apart from improvement in forecast accuracy measures of CPI inflation for the BRIC countries, another critical area that interests the policymakers is the knowledge of how various forms of structural uncertainties can influence the movement or complex dynamic behavior of different macroeconomic variables. The performance of FEWNet is superior to its counterparts in all three economies, except for China. This demonstrates that FEWNet is highly effective in handling complicated, non-stationary time series in forecasting tasks.

The paper is organized in the following way. Section 2 explains the macroeconomic series considered in this study, various data pre-processing strategies, and the causal association between the uncertainty indices and CPI inflation. Section 3 focuses on the proposed methodology with a detailed overview of its architectural design and Section 4 theoretically establishes the robustness of the method from an empirical risk minimization perspective. Section 5 discusses the experimental evaluation and the process of deriving a conformal prediction interval for the FEWNet framework. Finally, Section 6 ultimately wraps up the study by presenting a thorough analysis of the main discoveries and outlining potential future directions for the research.

2 Data and Preliminary Analysis

This work is premised on forecasting the monthly CPI inflation series for the four countries: Brazil, Russia, India, and China based on their historical data and various uncertainty indices EPU and GPRC¹. To evaluate the performance of our proposed method, we consider two forecast horizons of length 12 months and 24 months for each of the countries under study. In this section, we discuss the macroeconomic data considered in our analysis and their characteristics, along with the data preparation step (Section 2.1) and the causality analyses (Section 2.2) performed in this study. Furthermore, the implementable codes and the datasets used in this study are made available on [GitHub repository](#) for the reproducibility of the results.

2.1 Data Preparation and Global Characteristics

In our study, we consider the monthly CPI numbers for BRIC countries from 2003-01 to 2021-11 released by FRED (Federal Reserve Bank of St. Louis). These series are not adjusted for any seasonal patterns. The CPI series for all four countries are then converted to headline (HL) inflation numbers, described as “Year-on-Year” growth rate (“persistent rise in the general price level”) in the CPI series using the following approach:

$$\pi_{Jan}^{2003} = \left[\frac{CPI_{Jan}^{2003} - CPI_{Jan}^{2002}}{CPI_{Jan}^{2002}} \right] * 100\%,$$

where π_{Jan}^{2003} denotes the derived CPI inflation number for 2003-Jan, calculated using CPI values of 2003-Jan and 2002-Jan (prior year and same month). In addition to the CPI inflation, we also consider the impact of two uncertainty measures, namely the EPU and GPRC index, on the future projections of CPI inflation numbers for the BRIC countries. As part of the data pre-processing step, we perform the log transformation on the EPU series to stabilize its variance. Sequentially, we decompose the CPI inflation, log-transformed EPU, and GPRC series using the Hodrick and Prescott (HP) filter [49] and the Christiano-Fitzgerald (CF) random walk filter [50]. These economic filters play a vital role in extracting the trends and business cycles associated with the time series. Further details on the HP filter and CF filter are provided in Appendix 7.2.

In the analysis, we study the global features of the CPI inflation series, log-transformed EPU series, and GPRC series to identify their structural patterns and detect appropriate techniques for long-term forecasting. Primarily we focused on six popular time series characteristics, including skewness, kurtosis, non-linearity, long-range dependence, seasonality, and stationarity [51]. To assess the long-range dependency of the time series, we utilize the Hurst exponent. To analyze the non-linear characteristics of the series, we employ Tsay’s test and Keenan’s one-degree test for non-linearity. To determine the stationarity of the series, we conduct the Kwiatkowski–Phillips–Schmidt–Shin test. Lastly, to identify any seasonal patterns in the series, we apply the Ollech and Webel’s test. The results of the statistical features, summarized in Table 1, depict that most of the macroeconomic time series are non-stationary except for the GPRC series of Brazil and the CPI inflation data of China. The majority of these series are positively skewed except for the log-transformed EPU series of Russia. Furthermore, most of the economic time series exhibit non-linear patterns which plays a crucial role in selecting the appropriate modeling approach for the dataset. Additionally, based on Ollech and Webel’s seasonality test and the Hurst exponent we observe that all the series are non-seasonal and are characterized by long-range dependency. Moreover, the ACF and PACF plots of the CPI inflation series (presented in Table 2) depict the presence of serial autocorrelation. These inherent patterns of the CPI inflation series motivate the design and application of hybrid forecasting approaches for long-term forecasting.

2.2 Causality Analysis

This section explores the causal impact of log-transformed EPU and GPRC uncertainties on the CPI inflation series for the BRIC countries. Several statistical methods, such as the Granger causality test, cross-convergent

¹Two news-based measures of uncertainty are used in this study: the geopolitical risk uncertainty index (GPRC) [24] and the economic policy uncertainty index (EPU) of [19]. EPU stands for Economic Policy Uncertainty, which represents the likelihood of changes in monetary, fiscal, or regulatory policies that can impact the decision-making behavior of investors and consumers [19]. The geopolitical risk index [24] measures the occurrence of geopolitical events such as terrorism, local and regional political instability, political violence, coups d’état, territorial conflicts, and war. These events contribute to the uncertainty in the geopolitical landscape. Please refer to <http://www.policyuncertainty.com/> and <https://www.matteoiacoviello.com/gpr.htm> for more information on the EPU and GPRC index calculations.

Table 1: Global characteristics of the economic time series under study for BRIC countries.

Countries	Series	Skewness	Kurtosis	Non-Linearity	Long-Range Dependence	Seasonality	Stationarity
Brazil	CPI Inflation	1.67	3.57	Non-linear	0.73	Non-seasonal	Non-stationary
	log(EPU)	-0.9	0.29	Non-linear	0.77	Non-seasonal	Non-stationary
	GPRC	2.06	6.60	Non-linear	0.63	Non-seasonal	Stationary
Russia	CPI Inflation	0.28	-0.98	Linear	0.78	Non-seasonal	Non-stationary
	log(EPU)	-0.03	-0.12	Non-linear	0.79	Non-seasonal	Non-stationary
	GPRC	1.41	2.46	Linear	0.79	Non-seasonal	Non-stationary
India	CPI Inflation	0.71	0.17	Linear	0.82	Non-seasonal	Non-stationary
	log(EPU)	0.12	-0.47	Linear	0.80	Non-seasonal	Non-stationary
	GPRC	2.51	15.22	Non-linear	0.73	Non-seasonal	Non-stationary
China	CPI Inflation	0.82	1.08	Non-linear	0.69	Non-Seasonal	Stationary
	log(EPU)	0.23	-0.87	Non-linear	0.82	Non-seasonal	Non-stationary
	GPRC	1.28	1.51	Non-linear	0.80	Non-seasonal	Non-stationary

mappings, and transfer entropy, have been suggested in the literature to examine the causal relationship between two variables [52]. Nevertheless, the tests rely on certain data-level assumptions that are not met in the macroeconomic series analyzed in this work. In order to address this constraint, we employ wavelet coherence analysis (WCA) to examine the causal relationship between the series [53]. The WCA methodology offers a valuable method for examining the interconnection and simultaneous movement of two non-stationary signals in the time-frequency domain.

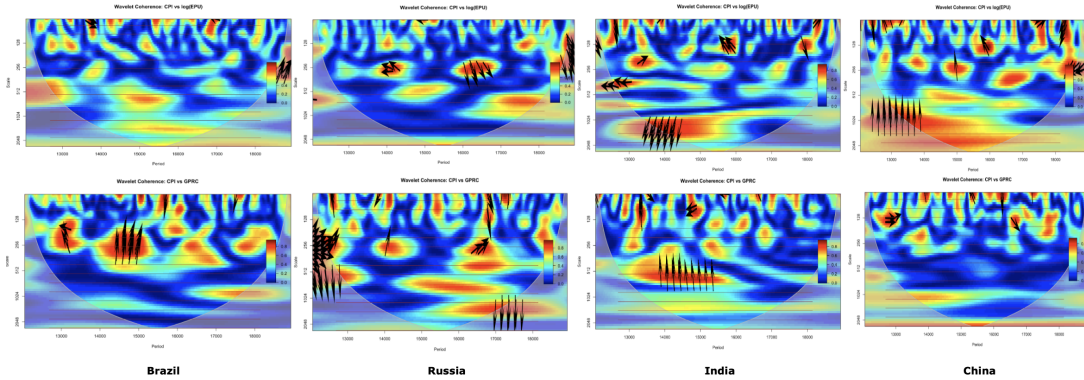


Figure 1: Wavelet coherence analysis plots - CPI inflation, log-transformed EPU (top) and CPI inflation, GPRC (bottom) for BRIC Countries

In the WCA plots, demonstrated in Figure 1, the first row depicts the WCA results between CPI inflation and log-transformed EPU series, and the second row shows the same for CPI inflation and GPRC series. In each of the plots horizontal axis measures the time, and the vertical axis shows the frequency dimension. Wavelet coherence represents the regions in the time-frequency domain where the two signals co-vary. In the plot, the transition from warmer colors (red) to colder colors (blue) indicates regions from higher coherence to lower coherence between the series. The arrow in the WCA plots indicates the lag phase relations between the analyzed signals. A zero-phase difference would hint toward the co-movement of the signals on any particular scale. The direction of an arrow has a specific connotation, with the arrows pointing to the right (left) indicating that the signals are in phase (anti-phase), i.e., the two signals are moving in the same direction or vice versa. As evident from the plots, there exists a significant causal relation between CPI inflation, log-transformed EPU, and GPRC series. This in turn, justifies the choice of EPU and GPRC as exogenous factors in forecasting the CPI inflation series of BRIC countries.

3 Proposed FEWNet Model

This section provides a comprehensive description of our proposed architecture, called the filtered ensemble wavelet neural network (FEWNet). FEWNet combines the maximal overlapping discrete wavelet transformation (MODWT) technique (explained in Appendix 7.1), economic filtering methods such as the Hodrick-Prescott (HP) filter and Christiano-Fitzgerald (CF) filter (explained in Appendix 7.2), and the autoregressive neural network with exogenous variables (ARNNx). The FEWNet framework is a sequential approach that initially decomposes the CPI inflation data into low-frequency (smooth) and \mathcal{K} high-frequency (detail) components using the scaling and wavelet filters of MODWT, as depicted in Figure 2. The ability of the transition and time-invariant MODWT approach to handle the non-stationary features of the time-dependent signal makes it a valuable tool in pre-processing the CPI inflation dataset. Simultaneously, to capture the economic uncertainties

Table 2: Training data for FEWNet including target series CPI inflation (blue) with corresponding ACF, PACF plots and exogenous variables log-transformed EPU (orange) and GPRC (grey) for the BRIC countries.

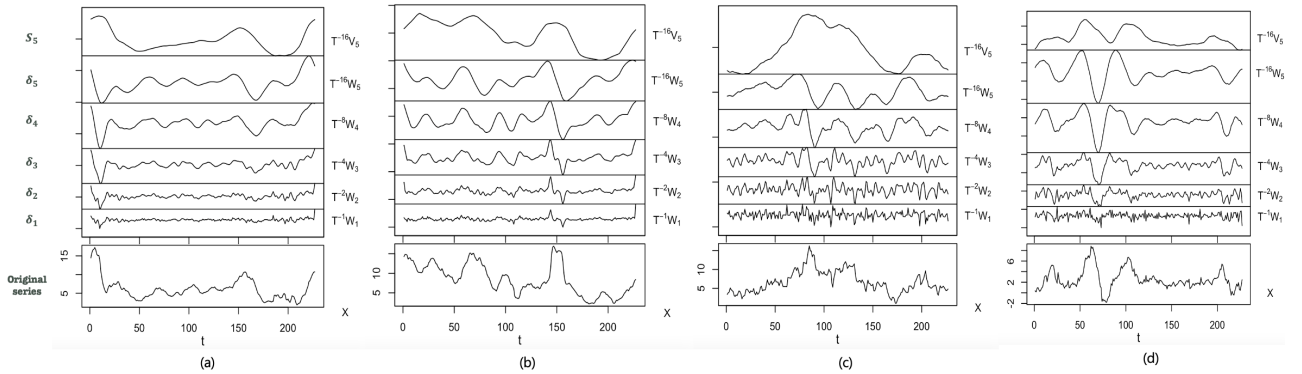
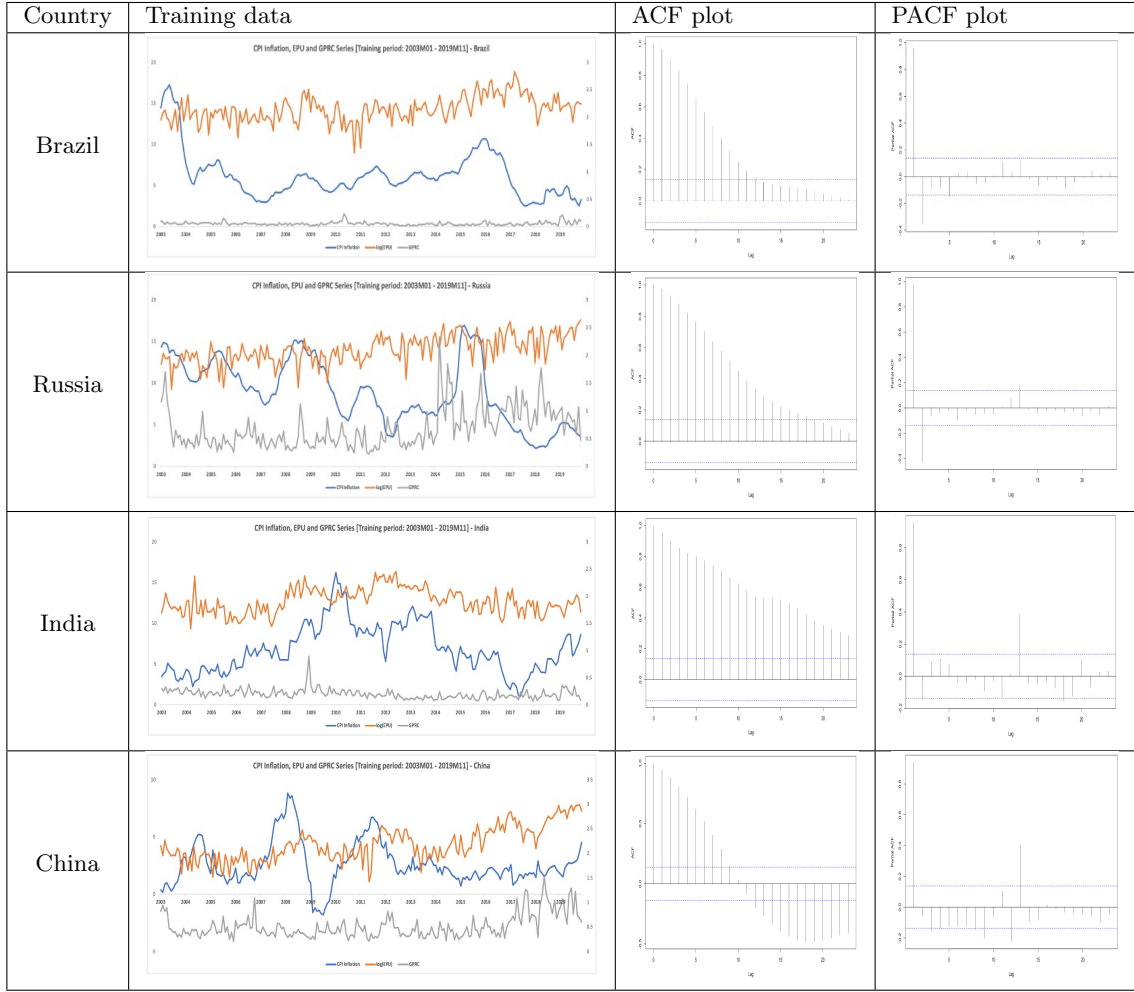


Figure 2: MODWT decomposition of the CPI Inflation series for (a) Brazil, (b) Russia, (c) India, and (d) China between the period Jan-2003 and Nov-2021. In these figures, $\delta_1, \delta_2, \dots, \delta_5$ and S_5 represent the details and smooth of the series generated by the MODWT-based MRA approach. The bottom chart in all the figures represents the original time series (CPI inflation) in actual frequency scale

of the time series, we apply the CF and HP filters on the CPI, log-transformed EPU, and GPRC series. The non-parametric CF filter efficiently captures the trend components, whereas the HP filter is suitable for identifying and modeling the business cycles. This long-term trend and the repetitive cyclical patterns have been found to provide significant information regarding the economic uncertainties that impact the future trajectories of the CPI inflation series.

The real-world Consumer Price Index (CPI) inflation series exhibit notable features, including non-stationarity, nonlinearity, and long-term dependence, as evidenced in Table 1. In order to accurately represent this non-uniform time series, we utilize MODWT decomposition using Daubechies orthogonal wavelets of length 2, namely the Haar filter. This transformation has the ability to identify the specific time and frequency components of signals, successfully distinguishing between long-range connections, non-stationarity, and patterns within the signals [54]. By utilizing the MODWT-based multi-resolution analysis (MRA) decomposition on the series Y_t , we derive a collection of $\mathcal{K} + 1$ distinct random variables called wavelet and scaling coefficients, which are not correlated with each other. In our suggested methodology, we employ separate neural networks within an ensemble framework to represent $\mathcal{K} + 1$ random variables, instead of employing the original CPI inflation series Y_t . These neural networks are specifically engineered and trained to effectively manage the intricacies linked to the wavelet coefficients. By employing this approach, we may efficiently tackle the non-linear nature observed in the Consumer Price Index (CPI) inflation data of the BRIC nations. In addition, in order to capture the temporal causal association between the input series and the exogenous variables ($X_{j,t}$, $j = 1, 2, \dots, 6$), we include them in each of the $\mathcal{K} + 1$ wavelet transformed series of Y_t in their corresponding neural networks. The forecasts produced by these $\mathcal{K} + 1$ neural networks are combined to determine the future dynamics of Y_t . The mathematical expression for the m -step ahead forecasts of Y_t , designated as $\hat{Y}_{\mathcal{N}+m}$, based on \mathcal{N} past data, is as follows:

$$\hat{Y}_{\mathcal{N}+m} = \hat{S}_{\mathcal{K},\mathcal{N}+m} + \sum_{\tilde{k}=1}^{\mathcal{K}} \hat{\delta}_{\tilde{k},\mathcal{N}+m}, \quad (1)$$

where $\hat{S}_{\mathcal{K},\mathcal{N}+m}$ and $\hat{\delta}_{\tilde{k},\mathcal{N}+m}$, $\tilde{k} = 1, 2, \dots, \mathcal{K}$ are the forecasts generated from the simultaneously computed neural networks of the smooth series $S_{\mathcal{K},t}$ and the details series $\delta_{\tilde{k},t}$, $\tilde{k} = 1, 2, \dots, \mathcal{K}$. Each of these $\mathcal{K} + 1$ neural networks consists of a feedforward design with three layers - the input layer with p nodes, one hidden layer with q nodes, and one output layer without any shortcut connections. The neural networks model incorporates $p - 6$ lagged observations of the wavelet coefficients, as well as one lagged observation for each of the six exogenous variables (X_j). These variables represent the trend and cycle information of CPI, log-transformed EPU, and GPRC. This setting allows the networks to generate one-step forward forecasts for the related series. Mathematically, the result obtained from each neural network after one iteration can be represented as:

$$\begin{aligned} \hat{\delta}_{\tilde{k},\mathcal{N}+1} &= \alpha_{0,\tilde{k}} + \sum_{i=1}^q \beta_{i,\tilde{k}} \sigma(\alpha_{i,\tilde{k}} + \beta'_{i,\tilde{k}} \vec{\delta}_{\tilde{k}} + \gamma'_{i,\tilde{k}} \underline{\mathbf{X}}); \tilde{k} = 1, 2, \dots, \mathcal{K} \\ \hat{S}_{\mathcal{K},\mathcal{N}+1} &= \alpha_0^S + \sum_{i=1}^q \beta_i^S \sigma(\alpha_i^S + \beta_i^{S'} \vec{S}_{\mathcal{K}} + \gamma_i^{S'} \underline{\mathbf{X}}), \end{aligned}$$

where $\vec{\delta}_{\tilde{k}}$ and $\vec{S}_{\mathcal{K}}$ denotes the $p - 6$ lagged observation of the corresponding wavelet coefficients and $\underline{\mathbf{X}}$ indicates a single lagged vector of exogenous variables, $\alpha_{0,\tilde{k}}, \alpha_{i,\tilde{k}}, \alpha_i^S$ are the bias terms, $\beta_{i,\tilde{k}}, \beta_i^S$ are the connection weights between hidden and output layer, $\gamma'_{i,\tilde{k}}, \gamma_i^{S'}$ are the weight vectors between the exogenous variables and the hidden layer, $\beta'_{i,\tilde{k}}, \beta_i^{S'}$ are the connection weights between lagged wavelet series and the hidden layer, and σ indicates the nonlinear activation function. Within our framework, we commence by assigning random initial values to the connection weights. Subsequently, we employ the gradient descent back-propagation approach to train these weights, as described in the work by [55]. The aforementioned technique produces a forecast that is one step ahead for each of the wavelets and scaling coefficients. In order to make forecasts for several future time steps, we incorporate the most recent predictions into the input layer instead of using the last observed value, and we continue this procedure recursively. Ultimately, we combine the predictions produced by each of the base models in an ensemble setup and derive the forecast for a for a desired time horizon.

The FEWNet algorithm consists of three hyperparameters: the level of MODWT decomposition (\mathcal{K}), the number of lagged observations in the input layer (p), and the number of hidden nodes (q). Prior research has indicated that selecting the appropriate level of wavelet decomposition (\mathcal{K}) is vital for distinguishing the genuine signal from noise in a complicated series [54, 56]. In order to limit the computational cost of the shift-invariant MODWT technique, we choose $\mathcal{K} = \lfloor \log_e(\text{length of training set}) \rfloor = \lfloor \log_e \mathcal{N} \rfloor$, where $\lfloor \cdot \rfloor$ denotes the floor function, following [34]. For specifying the number of previous lagged observations in the input layer we utilize the cross-validation strategy, and select p such that it minimizes the symmetric mean absolute percent error (SMAPE) of the validation set i.e.,

$$p = \underset{p}{\operatorname{argmin}} \frac{1}{|\mathcal{V}|} \sum_{t \in \mathcal{V}} \frac{2|\hat{Y}_t - Y_t|}{|\hat{Y}_t| + |Y_t|},$$

where \mathcal{V} indicates the validation set and Y_t and \hat{Y}_t are the original series and forecast at time t . Moreover, to stabilize the learning rate of the neural network, restrict overfitting, and to reduce the run-time of the

proposed FEWNet framework, we set the number of hidden nodes arranged in a single hidden layer as $q = \lceil \frac{p+1}{2} \rceil$ following [51,57]. The suggested FEWNet model is illustrated in Figure 3 using a schematic approach. The target time series is initially subjected to a MODWT-based MRA, resulting in multiple degrees of transformation, as shown in the figure. The economic uncertainties and geopolitical risk index series are filtered along with the CPI series using the CF filter and HP filter to generate the corresponding cycle (green circles) and trend (yellow circles) respectively. These six exogenous variables are then provided with the lagged wavelet series in the input layer of each of the $K + 1$ neural networks. The connection weights establish the connections between each input set and the hidden nodes, represented as lines with arrows. The results from the hidden layer are processed in the output layer, ultimately producing the forecast for the next step from the interconnected network. Ultimately, the future dynamics of the CPI inflation series are formed by producing multi-step ahead forecasts in a recursive fashion and then combining them in an ensemble. The utilization of wavelet decomposition to reveal the complex variability of the transformed series, and the subsequent modeling of these fluctuations with diverse economic filtered uncertainties using an auto-regressive neural network with auxiliary information within an ensemble framework, provides a valid rationale for naming the proposed model as FEWNet. The implementation methodology of the proposed FEWNet is outlined in Algorithm 1.

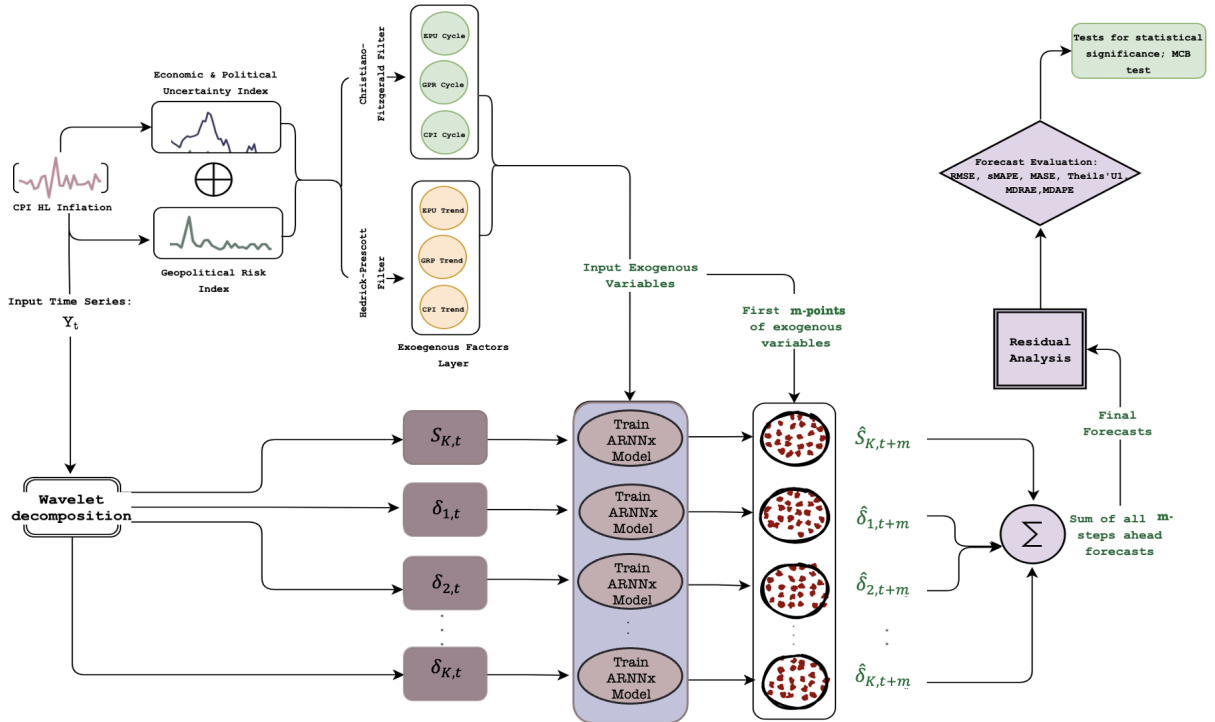


Figure 3: Illustration of the proposed FEWNet model

4 Empirical Risk Minimization

FEWNet utilizes wavelet decomposition as a filtering stage and combines it with autoregressive neural networks that incorporate exogenous variables. This combination allows for precise predictions of time series that are both non-stationary and nonlinear. Wavelet decomposition yields a hierarchical structure of new time series derived from the original time series, facilitating their modeling and forecasting. This section demonstrates that FEWNet effectively minimizes the empirical risk in comparison to classical methods, hence highlighting its practical relevance.

Let Y_t , ($t = 1, 2, \dots, \mathcal{N}$) be the observed time series (stationary if random) and we aim to forecast the values of $Y_{p+1}, Y_{p+2}, \dots, Y_{p+m}$ ($m \geq 1$ is the forecast step) using p observations iteratively. In regression setup, a functional relationship is established between Y_{p+m} and the input vector $[Y_1, Y_2, \dots, Y_p]$ by minimizing the predictive error. The optimal prediction sequence $\hat{Y}_{p+1}, \hat{Y}_{p+2}, \dots$ minimizes the generalization risk defined as follows

$$\mathcal{R}_{\text{Gen}} = \lim_{T \rightarrow \infty} \frac{1}{T} \sum_{p=1}^T \mathbb{E} \left[\left(\hat{Y}_{p+m} - Y_{p+m} \right)^2 \mid Y_p, Y_{p-1}, \dots \right],$$

Algorithm 1: Proposed FEWNet model

Input: A target time series $\{Y_t, t = 1, 2, \dots, \mathcal{N}\}$ indicating CPI inflation and exogenous series X_t comprising of log-transformed EPU, and GPRC.

Output: m (≥ 1) step-ahead forecast of the CPI inflation series Y_t .

Methodology:

- 1 Transform the target data vector (Y_t) into \mathcal{K} levels by applying MODWT with haar filter to generate a sequence of $\mathcal{K} + 1$ uncorrelated random variables indicating the local trend and high-frequency fluctuations of the series.
 - 2 Determine the value of \mathcal{K} as $\log_e(\mathcal{N})$, where \mathcal{N} represents the size of the training dataset.
 - 3 To quantify the economic uncertainty parameters of inflation data, apply CF and HP filters on the exogenous variables and the target variable to generate their corresponding cyclical and trend behavior, respectively.
for $\tilde{k} \leftarrow 1$ **to** \mathcal{K} **do**
 - Utilize an auto-regressive neural network to model the \tilde{k}^{th} detail series with $X_{j,t}, j = 1, 2, \dots, 6$.
 - Build a feed-forward neural network consisting of an input layer with p nodes, a hidden layer with q neurons, and an output layer.
 - Input one-lagged observation for each of the six filtered covariates along with $p - 6$ lagged values of the \tilde{k}^{th} detail series as input to the neural network. The neural network will then pass this input via q hidden neurons and generate the forecast for the next time step.
 - Determine the value of p that minimizes the SMAPE and set $q = \lceil \frac{p+1}{2} \rceil$, for stable learning architecture and shorter run time of the model.
 - return** *One-step forward forecast of the details series.*
 - 4 Apply an auto-regressive neural network to both the smooth series of Y_t and the exogenous variables, following the same definition used for the details series. Use this model to generate a forecast for future values.
 - 5 Create an ensemble framework to merge the forecasts produced from several series and get the final one-step forward prediction.
 - 6 Iteratively generate multi-step forward forecasts.
-

where $\hat{Y}_{p+m} = \mathbb{E}[Y_{p+m}|Y_p, Y_{p-1}, \dots]$. However, computation of \hat{Y}_{p+m} is difficult as the observed time series has \mathcal{N} observations (training samples). Therefore, we minimize the following empirical risk:

$$\mathcal{R}_{\text{Emp}} = \frac{1}{\mathcal{N}} \sum_{i=1}^{\mathcal{N}} (Y_i - \hat{Y}_i)^2, \quad (2)$$

where \hat{Y}_i is the prediction (expectations can be omitted for deterministic time series). In practical problems of economic time series forecasting, the relationship between \hat{Y}_{p+m} and the observed time sequence Y_p, Y_{p-1}, \dots is supposed to be nonlinear in nature. Thus, the inclusion of autoregressive neural networks (a set of feed-forward artificial neural networks designed specifically for predicting future values in time series data) for forecasting is justified in this exercise. The relationship can be estimated by

$$\hat{Y}_{p+m} = f(Y_p, Y_{p-1}, \dots, Y_1), \quad (3)$$

where f denotes an autoregressive neural network function. The model's order (p) is an essential parameter to estimate. Smaller values of p make the model training simple but miss the information about the past lagged values whereas larger values of p compel the model training hard resulting in a "curse of dimensionality". To avoid the issues of underfitting and overfitting, we use the ARNNx model, where we choose p by minimizing the SMAPE for the validation set. If f in Eq. (3) is a complex estimator (e.g., deep learning models such as transformers, deep MLP, etc), it will learn well on the training data but perform poorly on unseen test data. Application of MODWT decomposes the time series using low and high pass band filters iteratively resulting in a trend series and several detailed series (containing dynamics of the economic system at different scales). ARNNx is then trained to model the trend and detailed series and provide predictions for future values. The combined values of these MODWT-decomposed series provide a prediction of the original economic data. Although the main motivation for using wavelet decomposition on these economic time series is to enhance the predictive power, MODWT gives the smooth term $S_{\mathcal{K}}$ that contains the slowest dynamics (noise-free) and $\delta_{\tilde{k}}$ that contains system dynamics (noisy). The low-resolution data are frequently contaminated by noise. Consequently, training an ARNNx model on these time series is less challenging compared to the original time series. As \tilde{k} increases, the dynamics get slower, resulting in low-level detail series that consist solely of noise. To mitigate overfitting, one can assign a value of zero to their predictions.

Several recent works [56–59] have proposed to treat wavelet-decomposed time series independently. Another complicated approach will be to treat each series along with other series (treated as exogenous variables) but it results in increasing the dimensionality of the time series forecasting problem. In the current formulation we model $S_{\mathcal{K}}$ and other $\delta_{\tilde{k}}$, ($\tilde{k} = 1, 2, \dots, \mathcal{K}$) series using ARNNx models as follows:

$$\hat{S}_{\mathcal{K},p+m} = \hat{f}_0(S_{\mathcal{K},p}, S_{\mathcal{K},p-1}, \dots, S_{\mathcal{K},p-r_0}, \underline{X}) \text{ and } \hat{\delta}_{\tilde{k},p+m} = \hat{f}_{\tilde{k}}(\delta_{\tilde{k},p}, \delta_{\tilde{k},p-1}, \dots, \delta_{\tilde{k},p-r_{\tilde{k}}}, \underline{X}), \tilde{k} = 1, 2, \dots, \mathcal{K}. \quad (4)$$

The choice of \hat{f}_i ($i = 0, 1, 2, \dots, \mathcal{K}$) is related to the properties of the time series (nonlinear for this case). [57] proposed nonlinear ARNNx model and each \hat{f}_i may have the same order for r_i (we will use r for the rest) to decrease the model's complexity. The predictions are made as an equal-weighted combination of smooth and details predictions:

$$\hat{Y}_{p+m} = \hat{S}_{\mathcal{K},p+m} + \sum_{\tilde{k}=1}^{\mathcal{K}} \hat{\delta}_{\tilde{k},p+m}.$$

In this context, we establish empirical risk minimization (ERM) property for our proposed FEWNet framework. In statistical learning theory, ERM defines a family of learning models and provides theoretical bounds on their performances. This is useful since in practice we can't generalize how well a model will work (called true risk) due to not knowing the true data distribution. However, we can instead measure its performance on a known training data set (called empirical risk).

In FEWNet, we use ARNNx estimators $\hat{f}_0, \hat{f}_1, \dots, \hat{f}_{\mathcal{K}}$ with same order r having equal number of neurons in the network architecture. These estimators are obtained by simultaneously minimizing the following empirical risk:

$$\mathcal{R}_{\text{Emp}}^W = \frac{1}{\mathcal{N}} \sum_{p=1}^{\mathcal{N}} \left[\left(S_{\mathcal{K},p+m} - \hat{S}_{\mathcal{K},p+m} \right) + \sum_{\tilde{k}=1}^{\mathcal{K}} \left(\delta_{\tilde{k},p+m} - \hat{\delta}_{\tilde{k},p+m} \right) \right]^2. \quad (5)$$

Since ARNNx estimators can be expressed as a nonlinear combination of linear projections of lagged inputs for the CPI inflation series, the following result holds:

Proposition 1 *Let the autoregressive neural network (of order r) is applied to the original data (as in Eq. (3)) by minimizing the risk \mathcal{R}_{Emp} (as given in Eq. (2)) and FEWNet fits the ensemble model on the decomposed data by minimizing the empirical risk $\mathcal{R}_{\text{Emp}}^W$ (as in Eq. (5)), then we have*

$$\min \mathcal{R}_{\text{Emp}}^W \leq \min \mathcal{R}_{\text{Emp}}.$$

Proof 1 *Using Eq. (3) we write, the ARNNx estimator as follows*

$$\hat{f} = \alpha + \sum_{j'=1}^{q^*} \beta_{j'} \sigma(z_{j'}),$$

where $z_{j'} = \alpha^* + \sum_{i=1}^r \beta_{i,j'}^* y_i + \gamma^* \underline{X}$ where the parameters are estimated by minimizing Eq. (2). For FEWNet we have

$$\begin{aligned} \hat{f}_0 &= \alpha_0^S + \sum_{i=1}^q \beta_i^S \sigma(\alpha_i^S + \sum_{j_0=1}^r \beta_{i,j_0}^S S_{\mathcal{K},j_0} + \gamma_i^S \underline{X}) \\ \hat{f}_{\tilde{k}} &= \alpha_{0,\tilde{k}} + \sum_{i=1}^q \beta_{i,\tilde{k}} \sigma(\alpha_{i,\tilde{k}} + \sum_{j_{\tilde{k}}=1}^r \beta_{i,j_{\tilde{k}}} \delta_{\tilde{k},j_{\tilde{k}}} + \gamma'_{i,\tilde{k}} \underline{X}); \tilde{k} = 1, 2, \dots, \mathcal{K}. \end{aligned}$$

Using Jensen's inequality and Eq. (1), we get the \mathcal{R}_{Emp} definition domain is a subspace of $\mathcal{R}_{\text{Emp}}^W$

$$\mathcal{R}_{\text{Emp}} \leq \mathcal{R}_{\text{Emp}}^W.$$

Since \hat{f} is a linear combination of \hat{f}_0 and $\hat{f}_{\tilde{k}}$, ($\tilde{k} = 1, 2, \dots, \mathcal{K}$) with uniform weights and scaling (\tilde{g}_l) and wavelet (\tilde{h}_l) filter satisfies unit energy assumption and even length scaling assumption in MODWT i.e.,

$$\tilde{h}_l = -\tilde{g}_l \forall l \geq 1, \quad \tilde{h}_0 + \tilde{g}_0 = 1, \quad \tilde{h}_l = \tilde{g}_l = 0 \forall l \leq -1 \quad (6)$$

Similar results may hold for any other decomposition method satisfying the Eq. (6) in fact.

Remark 1 *However, it by no means guarantees the generalization risk reduction. In practical scenarios, the selection of the models for $\delta_{k,p}$ and $S_{\mathcal{K},p}$ would be crucial and can be done using cross-validation. Also the choice of r_i , ($i = 0, 1, \dots, \mathcal{K}$) may change the results in practice as can be thought of as a future advancement of this study. Our theoretical results show the robustness of the wavelet decomposed approaches in our proposal from an ERM perspective.*

5 Experimental Evaluation and Analysis of Results

We assessed the efficacy of the proposed FEWNet framework by comparing its performance to other baseline predictions derived from statistical, machine learning, and deep learning methodologies. In our experimental evaluation, we utilize a 5-fold time series cross-validation approach to train all the forecasting frameworks. We then generate forecasts for two different time horizons, specifically 12 months and 24 months, to demonstrate the generalizability of the setup. In this section, we briefly explain the baseline models (Section 5.1), evaluation metrics (Section 5.2), benchmark comparison, and experimental results (Section 5.3).

5.1 Baseline Models

We compared the FEWNet model and various baseline models, as well as a range of machine learning and deep learning algorithms that allow for the incorporation of exogenous factors. The evaluation incorporates the following competitive models:

- *Auto-regressive Integrated Moving Average with exogenous variable* (ARIMAx) model is widely used in time series forecasting [60]. The ARIMAx (p, d, q) framework captures the linear patterns of the time series by considering p previous values of the target series, q prior forecast errors, and historical values of the exogenous variable. This framework employs a differencing technique of order d to guarantee the stationarity of the data. The coefficients of the linear ARIMAx model are estimated by minimizing the Akaike information criterion (AIC) value.
- *Seasonal ARIMAx* (SARIMAx) is an extension of the ARIMAx model for seasonal time series datasets. The model has a similar architecture as the ARIMAx model with additional parameters for modeling the linear trend in the seasonal components of the series. Thus the SARIMAx (p, d, q)(P, D, Q, s) framework models the non-seasonal components of time series with parameters (p, d, q) and for the seasonal components of length s it utilizes the parameters (P, D, Q, s).
- *Auto-regressive Fractionally Integrated Moving Average with exogenous variable* (ARFIMAx) generalizes the classical ARIMAx model by allowing the value of the differencing parameter d to be a fraction i.e. $d \in (-0.5, 0.5)$. ARFIMAx (p, d, q) process has been widely studied to model and forecast time series exhibiting long-range dependence. As evident in Table 1, the CPI Inflation series along with the economic uncertainty indices exhibit long-range dependency, thus the choice of using the ARFIMAx model seems reasonable for our analysis to account for slowly decaying auto-correlations.
- *Deep-learning based Auto-regressive* (DeepAR) model is an advanced deep learning system designed specifically for forecasting time series data. This framework employs a recurrent neural network architecture to forecast future trajectories in a dataset that varies over time [61].
- *Neural Basis Expansion Analysis for Time Series* (NBeats) is a dense neural network structure explicitly developed for time series prediction problems. This model consists of many blocks, each composed of two main layers. The initial layer is responsible for modeling the time series to replicate previous observations and produce forecasts. Conversely, the second layer focuses on re-modeling the discrepancies between the actual and predicted values generated by the first layer and adjusting the forecasted figures. In our testing, we set the number of blocks as 2 to decrease the computational complexity of the framework.
- *Auto-regressive Distributed Lag* The autoregressive distributed lag (ARDL) model has been extensively employed in the field of econometrics to estimate the long-run and short-run dynamics of time series data [62]. The distributed lag components of the ARDL model are capable of simulating both the stationary and non-stationary time series components.

- *Lasso Regression* is a regularized linear regression model that handles overfitting using the L1 penalty. The penalty term involved in the loss function of the LASSO model helps in shrinking the coefficients of the regressor variables with limited predictive power, thus leading to feature selection.
- *Xtreme Gradient Boosting* (XGBoost) is a supervised machine learning algorithm that intends to predict the target variable through the ensemble of a set of weak learners [63]. These tree-based models are trained in a sequential fashion, where the model attempts to minimize the remaining error components of all the prior trees. During prediction, the sum of all the predicted values of the weak learners is reported. In our experimental analysis, we convert the forecasting task into a supervised prediction problem where the lagged inputs and the exogenous variables are the features and the subsequent forecast is the required label for the instance.
- *Temporal Fusion Transformer* (TFT) is a deep learning time series forecasting model that leverages the multi-head attention layer to capture the complex temporal dynamics of multiple time sequences. One of the key benefits of the TFT framework is its ability to model and forecast both univariate and multivariate time series simultaneously. Furthermore, the architecture is capable of incorporating additional information in the form of time-variant and static exogenous regressors. In our experimentation, we set the number of attention heads as 3.
- *Wavelet ARIMAx* (WARIMAx) is a modified version of the ARIMAx model that use the MODWT decomposition technique for the purpose of predicting time series data [59]. The model breaks down the signal that changes over time into several wavelet and smooth coefficients. It then uses an ARIMAx model to make predictions based on each of these series. The multi-step forecasts are derived by aggregating these candidate forecasts for a desired horizon.
- *Auto-regressive Neural Network with exogenous variable* (ARNNx) is a generalization of the classical feed-forward neural network model for the auto-regressive time series process [64]. This model utilizes previous observations of the target time series and the exogenous variables as input to the network. The ARNNx model comprises a single hidden layer positioned between the input and output layers. The ARNNx (p, k) model uses p -lagged input values from the input layers and passes them via k neurons in the hidden layer. The value of k is typically calculated by the formula $k = \lceil \frac{p+1}{2} \rceil$, where p is a given parameter. This approach helps mitigate overfitting and maintain a stable learning architecture [51]. The model gets initialized with random values and trained using the gradient descent back-propagation approach [55].

5.2 Evaluation Metrics

In our study, we have considered five evaluation metrics to assess the performance of the proposed forecaster and the baseline models in generating the 12-month and 24-month ahead forecasts of the CPI inflation series for the BRIC countries. These metrics include the Root Mean Square Error (RMSE), Mean Absolute Scaled Error (MASE), Symmetric Mean Absolute Percentage Error (SMAPE), Theils' U1 measure, Median Relative Absolute Error (MDRAE), and Median Absolute Percentage Error (MDAPE). The mathematical expression of these metrics is provided as follows:

$$\text{RMSE} = \sqrt{\frac{1}{m} \sum_{t=1}^m (y_t - \hat{y}_t)^2}; \quad \text{MASE} = \frac{\sum_{t=D+1}^{D+m} |\hat{y}_t - y_t|}{\frac{m}{D-S} \sum_{t=S+1}^D |y_t - y_{t-S}|}; \quad \text{SMAPE} = \frac{1}{m} \sum_{t=1}^m \frac{|\hat{y}_t - y_t|}{(|\hat{y}_t| + |y_t|)/2} \times 100\%$$

$$\text{Theils U1} = \frac{\sqrt{\frac{1}{m} \sum_{t=1}^m (y_t - \hat{y}_t)^2}}{\sqrt{\frac{1}{m} \sum_{t=1}^m y_t^2} \sqrt{\frac{1}{m} \sum_{t=1}^m \hat{y}_t^2}}; \quad \text{MDRAE} = \text{median}_{t=1, \dots, m} \frac{|y_t - \hat{y}_t|}{y_t - \hat{y}_t^R}; \quad \text{and} \quad \text{MDAPE} = \text{median}_{t=1, \dots, m} \frac{|y_t - \hat{y}_t|}{y_t} \times 100\%;$$

where y_t is the ground truth, \hat{y}_t is the forecast of the corresponding model, \hat{y}_t^R is the naive forecast at time t , and m is the forecast horizon. By convention, the model with the lowest value of the error metric is considered as the best-performing model [51, 57].

5.3 Experimental results and baseline comparison

This section focuses on the implementation and effectiveness of the proposed FEWNet architecture in forecasting the Consumer Price Index (CPI) inflation series of the BRIC countries. In order to conduct a thorough assessment, we compare the performance of FEWNet to various cutting-edge algorithms. The FEWNet model is implemented using the R statistical software. The MODWT technique is first implemented using the *modwt* function from the 'wavelets' package. This function decomposes the training data into wavelet and scaling

coefficients using the pyramid algorithm with the ‘haar’ filter. The determination of the number of decomposition levels is done conventionally as the floor function of $\log_e(\text{length}(\text{train}))$ [34]. In the subsequent phase, each wavelet (details) and scaling (smooth) coefficient series is modeled with trend and cycle information from the log-transformed EPU, GPRC, and CPI data obtained through economic filters. This is achieved using an ARNNx model fitted with the *nnetar* function from the ‘forecast’ package in R. To select the number of inputs (p) for the individual networks, a time series cross-validation approach is applied with a search range of 1-24. Subsequently, these p inputs are processed through $k = (p + 1)/2$ hidden nodes arranged in a single hidden layer. This process generates one-step ahead forecasts for the individual series, which are aggregated to produce the final forecast. The framework iteratively generates multi-step ahead forecasts. The hyperparameters of the FEWNet(p, k) algorithm used in this study are summarized in Table 3. Furthermore, for implementing classical forecasters such as ARIMAx, SARIMAx, ARDL, ARFIMAx, and WARIMAx, the ‘statsmodels’ library in Python is employed. Deep learning models, including DeepAR, NBeats, and TFT, are implemented using the ‘darts’ library in Python. The machine learning frameworks like Lasso and XGBoost are implemented using the ‘skforecast’ package in Python.

Country	Algorithm	$(p, k)_{FH=12M}$	$(p, k)_{FH=24M}$
Brazil	FEWNet	(6,5)	(18,11)
Russia	FEWNet	(1,2)	(18,11)
India	FEWNet	(18,11)	(12,8)
China	FEWNet	(18,11)	(12,8)

Table 3: Model parameters: (p, k) of FEWNet for BRIC countries across different forecast – horizons. The table shows optimal parameter combinations for 12-month and 24-month rolling window forecasts of CPI inflation.

After implementing the proposed FEWNet model and other baseline architectures, we generate forecasts for the specified time horizons. Tables 4 and 5 display the performance of the models for the semi-long term (12-month) and long-term (24-month) timeframes, respectively, using out-of-sample data. The error metrics reported in the tables indicate that, in the majority of forecasting tasks, the proposed FEWNet framework outperforms the baseline models. In the semi-long term forecasting of Brazil, the FEWNet model significantly reduces the RMSE metric of the ARNNx model. This improvement in model performance is attributed to the application of wavelet decomposition in the FEWNet model. A similar conclusion is supported by other accuracy metrics. For the CPI inflation series of Russia, while the DeepAR model provides the best forecasts among the baseline models, the FEWNet model’s forecasts closely align with the ground truth. The 12-month ahead CPI inflation forecasts of India generated by the proposed architecture show substantial improvement over the best-performing NBeats and WARIMAx models. When forecasting the CPI series of China, the NBeats model competes with the FEWNet architecture, with the former exhibiting the best accuracy for all metrics except SMAPE. The Chinese Consumer Price Index (CPI) series demonstrates a pattern of stable trends (trend-stationary). While the wavelet-decomposition approach is commendable for tackling structural volatility and non-stationarity, its efficacy may be restricted when applied to trend-stationary or covariance stationary series. Consequently, it may not outperform other statistical or machine-learning methods when used on inherently stationary series (a property that is not prevalent for most macroeconomic variables). This explains the cause of the somewhat competitive or less efficient performance of FEWNet in predicting Chinese inflation numbers. In long-term forecasting, the FEWNet architecture consistently outperforms baseline models for all countries except China, where the NBeats model demonstrates more accurate forecasts of the CPI series. Throughout the experimental evaluations, the importance of wavelet transformation and the economic filtered auxiliary information becomes evident in efficiently capturing both time and frequency-level dynamics of the time series. While machine learning and deep learning models generally produce competitive performances for semi-long forecast horizons, their effectiveness diminishes significantly over the long-term horizon. In contrast, the FEWNet model consistently performs well over both horizons, demonstrating its generalizability. Additionally, the wavelet decomposition of the FEWNet approach proves to be a suitable technique for modeling time-frequency information, especially for target variables exhibiting non-stationary behavior (unlike China). Given that most economic time series follow a non-stationary trajectory, the FEWNet approach emerges as an ideal framework for their long-term forecasting even in the presence of structural volatility.

5.4 Statistical significance of the results

In this section, we assess the effectiveness of different forecasting models in terms of the statistical significance of measurement error differences using the model-agnostic multiple comparisons with the best (MCB) procedure

Table 4: Performance of the proposed FEWNet model in comparison to baseline forecasting techniques for 12 months ahead forecasts with exogenous factors EPU, and GPRC (best results are made **bold**).

Country	Metrics	DeepAR	ARNNx	NBeats	ARFIMAx	SARIMAx	ARIMAx	LR	ARDL	XGBoost	TFT	WARIMAx	Proposed FEWNet
Brazil	<i>RMSE</i>	3.41	2.23	2.95	4.67	2.37	2.69	2.19	3.26	2.40	5.41	3.13	1.30
	<i>MASE</i>	5.24	3.32	4.41	7.49	3.77	4.29	3.45	5.57	3.62	8.51	4.88	1.80
	<i>SMAPE(%)</i>	37	25	34	68	29	33	26	52	27	85	39	12
	<i>Theil's U₁</i>	0.20	0.14	0.22	0.38	0.16	0.19	0.14	0.25	0.17	0.48	0.23	0.09
	<i>MDRAE</i>	4.42	2.45	5.22	8.38	3.84	4.44	3.70	5.24	4.41	9.26	5.45	1.97
	<i>MDAPE</i>	0.30	0.20	0.34	0.59	0.27	0.30	0.23	0.40	0.26	0.46	0.39	0.10
Russia	<i>RMSE</i>	2.00	4.16	2.49	12.68	6.65	7.80	4.45	3.65	6.21	3.87	3.72	0.88
	<i>MASE</i>	4.66	10.17	5.63	33.84	17.62	20.26	11.28	9.67	16.06	9.96	9.44	2.21
	<i>SMAPE(%)</i>	26	46	38	100	69	76	48	44	63	81	44	13
	<i>Theil's U₁</i>	0.15	0.25	0.23	0.50	0.34	0.38	0.26	0.22	0.33	0.42	0.23	0.07
	<i>MDRAE</i>	4.23	10.20	5.00	40.54	18.31	23.76	12.70	12.14	15.49	7.57	9.15	2.88
	<i>MDAPE</i>	0.33	0.51	0.32	1.97	1.05	1.22	0.71	0.57	0.99	0.59	0.56	0.11
India	<i>RMSE</i>	3.55	1.69	1.09	1.86	2.27	2.31	2.46	1.88	1.69	1.67	1.19	0.88
	<i>MASE</i>	6.61	2.68	1.82	2.92	3.72	3.88	4.19	2.96	3.07	2.35	2.00	1.41
	<i>SMAPE(%)</i>	52	33	22	28	51	54	58	38	38	24	23	15
	<i>Theil's U₁</i>	0.27	0.21	0.12	0.17	0.29	0.30	0.33	0.23	0.21	0.16	0.13	0.09
	<i>MDRAE</i>	9.18	2.18	1.70	2.43	3.91	5.16	4.26	2.37	3.93	1.86	2.46	1.22
	<i>MDAPE</i>	0.68	0.26	0.20	0.38	0.30	0.34	0.44	0.30	0.36	0.15	0.22	0.15
China	<i>RMSE</i>	1.33	2.01	0.90	10.45	4.54	5.21	2.35	3.34	0.99	2.11	4.85	1.70
	<i>MASE</i>	1.73	2.76	1.18	15.68	6.68	7.67	3.24	4.75	1.25	2.77	7.18	1.93
	<i>SMAPE(%)</i>	94	111	116	171	146	150	115	132	99	153	149	85
	<i>Theil's U₁</i>	0.42	0.49	0.34	0.83	0.68	0.71	0.53	0.62	0.35	0.80	0.70	0.43
	<i>MDRAE</i>	1.29	2.60	1.28	15.94	7.27	8.04	3.41	5.17	1.25	3.95	7.38	1.75
	<i>MDAPE</i>	1.66	1.70	0.87	14.68	6.80	7.67	2.26	5.07	0.93	1.99	7.21	0.99

Table 5: Performance of the proposed FEWNet model in comparison to baseline forecasting techniques for 24 months ahead forecasts with exogenous factors EPU, and GPRC (best results are made **bold**).

Country	Metrics	DeepAR	ARNNx	NBeats	ARFIMAx	SARIMAx	ARIMAx	LR	ARDL	XGBoost	TFT	WARIMAx	Proposed FEWNet
Brazil	<i>RMSE</i>	6.16	3.56	3.11	4.27	4.13	4.49	3.67	2.86	2.56	3.58	4.11	2.31
	<i>MASE</i>	11.45	6.68	5.10	6.04	7.67	8.27	6.93	5.23	3.62	6.11	5.93	4.12
	<i>SMAPE(%)</i>	91	57	47	58	64	58	58	47	40	55	57	39
	<i>Theil's U₁</i>	0.45	0.27	0.29	0.47	0.32	0.36	0.27	0.23	0.21	0.31	0.45	0.19
	<i>MDRAE</i>	12.66	6.81	5.60	3.67	9.31	8.31	7.49	5.87	5.11	6.85	3.76	4.84
	<i>MDAPE</i>	0.86	0.60	0.48	0.36	0.56	0.65	0.70	0.44	0.41	0.50	0.39	0.36
Russia	<i>RMSE</i>	3.26	6.12	5.26	11.69	9.90	9.49	6.97	6.67	2.16	2.72	5.22	2.24
	<i>MASE</i>	8.39	18.32	14.63	35.12	28.78	27.25	20.31	19.75	5.10	7.00	15.03	5.28
	<i>SMAPE(%)</i>	51	81	66	112	101	98	84	84	36	44	72	27
	<i>Theil's U₁</i>	0.28	0.38	0.34	0.54	0.51	0.50	0.42	0.40	0.25	0.24	0.35	0.18
	<i>MDRAE</i>	8.29	21.94	15.12	41.21	30.43	26.85	24.53	24.47	4.76	7.21	17.53	3.51
	<i>MDAPE</i>	0.44	1.33	1.09	2.49	2.02	1.87	1.38	1.47	0.35	0.43	1.14	0.38
India	<i>RMSE</i>	1.86	2.22	4.18	2.72	2.16	2.02	2.36	2.53	1.95	6.17	2.35	1.04
	<i>MASE</i>	2.68	2.90	5.83	4.20	3.02	2.83	3.61	2.98	2.80	9.48	3.39	1.49
	<i>SMAPE(%)</i>	26	35	46	38	34	31	47	37	33	65	37	17
	<i>Theil's U₁</i>	0.15	0.23	0.29	0.21	0.21	0.19	0.26	0.26	0.20	0.37	0.21	0.10
	<i>MDRAE</i>	3.25	4.31	6.22	6.46	4.02	4.07	4.21	2.12	4.28	13.47	3.70	1.42
	<i>MDAPE</i>	0.31	0.24	0.49	0.42	0.30	0.28	0.41	0.21	0.26	1.07	0.40	0.14
China	<i>RMSE</i>	1.71	1.85	1.43	18.37	3.48	4.04	1.59	2.00	2.87	2.05	7.40	2.01
	<i>MASE</i>	1.95	2.15	1.75	25.72	4.23	5.05	1.89	2.33	3.12	2.42	10.17	2.37
	<i>SMAPE(%)</i>	81	77	77	168	102	109	75	79	115	100	139	82
	<i>Theil's U₁</i>	0.40	0.34	0.27	0.81	0.48	0.51	0.30	0.34	0.65	0.46	0.64	0.36
	<i>MDRAE</i>	1.53	2.32	1.60	26.02	4.43	4.99	2.09	2.51	2.68	2.32	10.88	2.50
	<i>MDAPE</i>	0.57	0.85	0.63	11.56	2.05	2.41	0.55	0.99	1.14	0.84	4.84	0.84

[65]. This non-parametric test computes the average rank for each of the \mathcal{M} forecasters based on their ex-ante accuracy across \mathcal{D} datasets and identifies the model with the minimum average rank as the ‘best’ performing technique. The MCB test determines critical distances (CD) for each algorithm as $\Theta_\alpha \sqrt{\frac{\mathcal{M}(\mathcal{M}+1)}{6\mathcal{D}}}$, where Θ_α is the critical value of the Tukey distribution at level α , and it considers the CD of the best-performing model as the reference value for the test. Following the MCB test, we calculate the average rank of the algorithm and present the results of the MCB test for the RMSE metric in Figure 4. The plot reveals that the FEWNet framework has achieved the lowest mean rank of 2.12 among all competing algorithms for both forecast horizons. Therefore, it is deemed to be the best-performing model, followed by NBeats (4.38), XGBoost (4.50), ARNNx (5.25), and so forth. Furthermore, the upper limit of the critical distance for the FEWNet model (shown by the shaded area in the graphs) acts as the reference value for the test. When comparing SARIMAx, ARIMAx, and ARFIMAx to the baseline, it is observed that their critical intervals are much higher than the reference value and do not coincide with FEWNet. This indicates that their forecast performance is notably worse than the FEWNet approach. Our analysis underscores the statistical significance of the performance difference and the superiority of the proposed FEWNet model across datasets and forecast horizons. Moreover, the test establishes that FEWNet consistently and significantly outperforms other baseline models, as well as various machine learning or deep learning models.

5.5 Conformalized Prediction Intervals

Next, we focus on quantifying the uncertainty associated with the forecast generated by the FEWNet approach using a conformal prediction interval. The non-parametric conformal prediction approach, introduced in [66], is a set of methods that usually take an uncertainty score and turn it into a probabilistic band, including the true outcome. In other words, this framework converts point estimations into a prediction region. One of the significant advantages of conformal prediction intervals is that this model-agnostic procedure guarantees

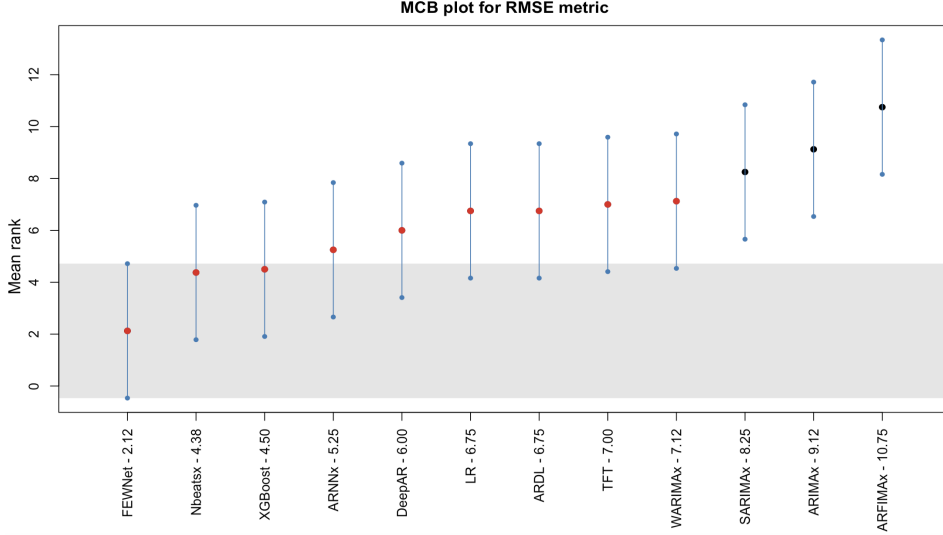


Figure 4: Visualization of the multiple comparisons with best (MCB) analysis for (a) Brazil, (b) Russia, (c) India (d) China [BRIC] countries: In the figure, for example in (a) FEWNet- 2.12 means that the average rank of the proposed algorithm FEWNet based on RMSE error metric is 2.12, the same explanation applies to other countries and algorithms

coverage. In the time series setup, this method generates the prediction interval by leveraging the sequential ordering of the data. Given the training set $\{Y_t, \tilde{X}_t\}_{t=1}^N$ where Y_t is the target series, and \tilde{X}_t is the set of features, including lagged historical values of Y_t and the covariates, we fit the FEWNet framework and an uncertainty model $\hat{\Xi}$ on \tilde{X}_t to generate a scalar notion of uncertainty. The conformal score \mathcal{S}_t can be calculated as:

$$\mathcal{S}_t = \frac{|Y_t - \text{FEWNet}(\tilde{X}_t)|}{\hat{\Xi}(\tilde{X}_t)}$$

Owing to the sequential nature of the data points, the conformal quantile for time series data can be calculated as a weighted conformal technique with a fixed κ -sized window $\omega_{t'} = \mathbb{1}\{t' \geq t - \kappa\}, \forall t' < t$. This now yields the quantile values as,

$$\hat{Q}_t = \text{inf} \left\{ q : \frac{1}{\min(\kappa, t' - 1) + 1} \sum_{t'=1}^{t-1} \mathcal{S}_{t'} \mathbb{1}(t' \geq t - \kappa) \geq 1 - \alpha \right\}$$

Based on these weights-adjusted quantiles, the prediction interval at each time step t can be computed as,

$$\mathbb{C}(\tilde{X}_t) = \left[\text{FEWNet}(\tilde{X}_t) - \hat{Q}_t \hat{\Xi}(\tilde{X}_t), \text{FEWNet}(\tilde{X}_t) + \hat{Q}_t \hat{\Xi}(\tilde{X}_t) \right].$$

In this section, we present the conformal prediction intervals for the 24-month ahead CPI inflation forecasts generated by the FEWNet model using the validation data points (2019-12 to 2021-11). The conformal prediction interval of the FEWNet framework, calculated based on the forecast estimates and residuals for the validation set, is demonstrated in Figure 5 along with the point estimate of the forecast produced by FEWNet and the best-performing baseline models for the BRIC countries. As observed in the figure the prediction intervals vary in width across different datasets. For instance, in the case of the 24-month forecast for Brazil, the width of the interval averages around 8.18, for Russia, it hovers around 7.93, for India, it reaches the minimum of 3.88; and for China, it averages around 7.60. A similar analysis of the conformal prediction intervals for the semi-long term forecast horizon is provided in Appendix 7.3. The overall analysis thus demonstrates a form of uncertainty quantification for the forecast of CPI inflation series for BRIC countries and shows the structural shift in the measurement of prediction uncertainty across different countries.

6 Conclusion and Discussion

Historically, emerging economies have exhibited higher and more enduring inflation rates when compared to developed countries. Most emerging economies have implemented an inflation-targeting monetary policy frame-

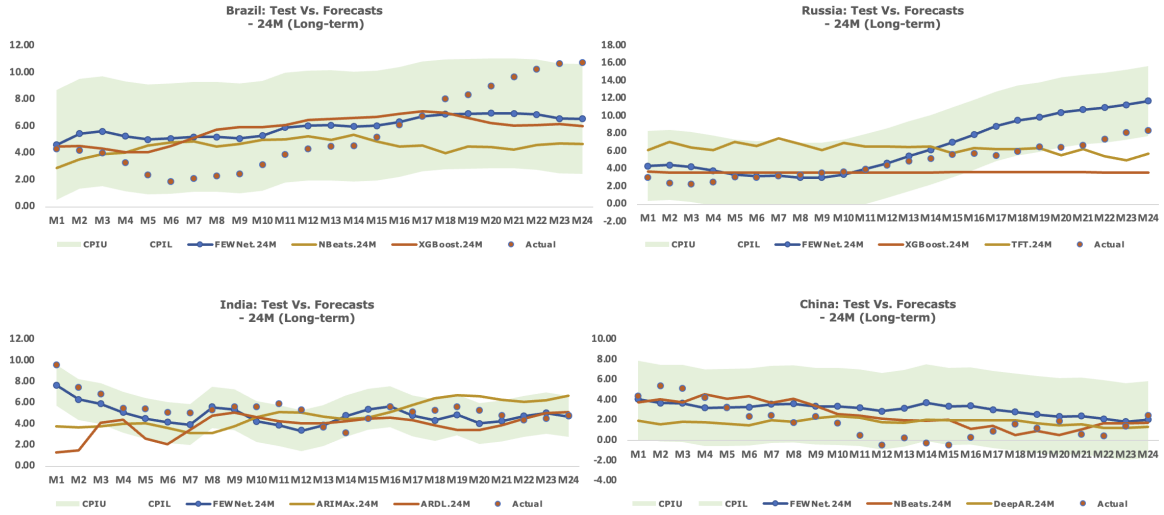


Figure 5: The plot shows the ground truth CPI inflation data (red dots), forecast generated by the best (yellow) and second-best (orange) baseline models for each country, conformal prediction interval (green shaded), and forecast (blue) generated by the FEWNet model for the long-term forecast horizon in BRIC Countries

work in which inflation serves as the intermediate target. This paper outlines a novel machine learning framework, namely FEWNet, that combines the MODWT process with the ARNNx model for long-term CPI inflation forecasting for the BRIC countries under macroeconomic and geopolitical uncertainties. The proposed method demonstrates consistent performances for 3 out of 4 major BRIC economies for both the semi-long run and long-run forecast horizons. Since the CPI inflation data of China presents a stationary behavior, our proposal failed to outperform benchmark forecasters that work exceptionally well on stationary time series. Moreover, for Brazil, Russia, and India it produces the most accurate performance, outperforming the classical and SOTA machine learning or deep learning algorithms. We also present a framework for time series feature engineering using different economic filters (HP and CF band-pass filters) that can be very easily leveraged in the proposed architecture, which supports the inclusion of exogenous regressors within its flexible design. A combination of the multiresolution analysis and autoregressive neural networks are used to predict nonlinearity, nonstationarity, and non-gaussian time series of inflation. MODWT decomposition produces new time series that contains system and slow dynamics that easily separate signal from noise. Each time series is further modeled with ARNNx. Theoretically, we show that under certain conditions, the proposed FEWNet reduces the empirical risk, resulting in improved forecast accuracy.

Although FEWNet is designed to predict CPI inflation of BRIC countries, it can be seamlessly extended for developed countries and can include other uncertainty variables like Twitter-based uncertainties, financial stress indicators, world uncertainty index, etc. This framework can also be leveraged for forecasting other macroeconomic variables like GDP, gold price, unemployment rate, and others. The FEWNet framework is more effective for generating forecasts for non-stationary and non-linear time series data that are evident in macroeconomics; therefore, it can potentially serve as a viable alternative to forecasting strategy for central banks. In light of our results, further analysis of the FEWNet’s performance in predicting other macroeconomic time series as well as inflation in a multivariate forecasting setting seems to be a promising avenue for future research.

References

- [1] James H Stock and Mark W Watson. Why has us inflation become harder to forecast? *Journal of Money, Credit and banking*, 39:3–33, 2007.
- [2] Bhanu Pratap and Shovon Sengupta. Rbi working paper series no. 04 macroeconomic forecasting in india: Does machine learning hold the key to better forecasts? 2019.
- [3] Jon Faust and Jonathan H Wright. Forecasting inflation. In *Handbook of economic forecasting*, volume 2, pages 2–56. Elsevier, 2013.

- [4] Aaron Smalter Hall and Thomas R Cook. Macroeconomic indicator forecasting with deep neural networks. *Federal Reserve Bank of Kansas City Working Paper*, (17-11), 2017.
- [5] Emi Nakamura. Inflation forecasting using a neural network. *Economics Letters*, 86(3):373–378, 2005.
- [6] M Ali Choudhary and Adnan Haider. Neural network models for inflation forecasting: an appraisal. *Applied Economics*, 44(20):2631–2635, 2012.
- [7] Xiaohong Chen, Jeffrey Racine, and Norman R Swanson. Semiparametric arx neural-network models with an application to forecasting inflation. *IEEE Transactions on neural networks*, 12(4):674–683, 2001.
- [8] Peter McAdam and Paul McNelis. Forecasting inflation with thick models and neural networks. *Economic Modelling*, 22(5):848–867, 2005.
- [9] Anna Almosova and Niek Andresen. Nonlinear inflation forecasting with recurrent neural networks. *Journal of Forecasting*, 42(2):240–259, 2023.
- [10] Oren Barkan, Jonathan Benchimol, Itamar Caspi, Eliya Cohen, Allon Hammer, and Noam Koenigstein. Forecasting cpi inflation components with hierarchical recurrent neural networks. *International Journal of Forecasting*, 39(3):1145–1162, 2023.
- [11] Marcelo C Medeiros, Gabriel FR Vasconcelos, Álvaro Veiga, and Eduardo Zilberman. Forecasting inflation in a data-rich environment: the benefits of machine learning methods. *Journal of Business & Economic Statistics*, 39(1):98–119, 2021.
- [12] Sendhil Mullainathan and Jann Spiess. Machine learning: an applied econometric approach. *Journal of Economic Perspectives*, 31(2):87–106, 2017.
- [13] Gustavo Silva Araujo and Wagner Piazza Gaglianone. Machine learning methods for inflation forecasting in brazil: New contenders versus classical models. *Latin American Journal of Central Banking*, 4(2):100087, 2023.
- [14] Evgeny Pavlov. Forecasting inflation in russia using neural networks. *Russian Journal of Money and Finance*, 79(1):57–73, 2020.
- [15] Byron Botha, Rulof Burger, Kevin Kotzé, Neil Rankin, and Daan Steenkamp. Big data forecasting of south african inflation. *Empirical Economics*, 65(1):149–188, 2023.
- [16] Önder Özgür and Uğur Akkoç. Inflation forecasting in an emerging economy: selecting variables with machine learning algorithms. *International Journal of Emerging Markets*, 17(8):1889–1908, 2021.
- [17] Nicholas Bloom. The impact of uncertainty shocks. *econometrica*, 77(3):623–685, 2009.
- [18] Nicholas Bloom. Fluctuations in uncertainty. *Journal of economic Perspectives*, 28(2):153–176, 2014.
- [19] Scott R Baker, Nicholas Bloom, and Steven J Davis. Measuring economic policy uncertainty. *The quarterly journal of economics*, 131(4):1593–1636, 2016.
- [20] Paul M Jones and Eric Olson. The time-varying correlation between uncertainty, output, and inflation: Evidence from a dcc-garch model. *Economics Letters*, 118(1):33–37, 2013.
- [21] Sylvain Leduc and Zheng Liu. Uncertainty shocks are aggregate demand shocks. *Journal of Monetary Economics*, 82:20–35, 2016.
- [22] Valentina Colombo. Economic policy uncertainty in the us: Does it matter for the euro area? *Economics Letters*, 121(1):39–42, 2013.
- [23] Mehmet Balcilar, Rangan Gupta, and Charl Jooste. Long memory, economic policy uncertainty and forecasting us inflation: a bayesian varfima approach. *Applied Economics*, 49(11):1047–1054, 2017.
- [24] Dario Caldara and Matteo Iacoviello. Measuring geopolitical risk. *American Economic Review*, 112(4):1194–1225, 2022.
- [25] Opeoluwa Adeniyi Adeosun, Mosab I Tabash, Xuan Vinh Vo, and Suhaib Anagreh. Uncertainty measures and inflation dynamics in selected global players: a wavelet approach. *Quality & Quantity*, 57(4):3389–3424, 2023.
- [26] Christina Anderl and Guglielmo Maria Caporale. Asymmetries, uncertainty and inflation: evidence from developed and emerging economies. *Journal of Economics and Finance*, pages 1–34, 2023.

- [27] Riza Demirer and Rangan Gupta. Policy uncertainty and stock market volatility revisited: The predictive role of signal quality afees a. salisu. 2022.
- [28] Li Liu and Tao Zhang. Economic policy uncertainty and stock market volatility. *Finance Research Letters*, 15:99–105, 2015.
- [29] Adam T Jones and William H Sackley. An uncertain suggestion for gold-pricing models: The effect of economic policy uncertainty on gold prices. *Journal of Economics and Finance*, 40:367–379, 2016.
- [30] Juha Junttila and Juuso Vataja. Economic policy uncertainty effects for forecasting future real economic activity. *Economic Systems*, 42(4):569–583, 2018.
- [31] Saud Asaad Al-Thaqeb and Barrak Ghanim Algharabali. Economic policy uncertainty: A literature review. *The Journal of Economic Asymmetries*, 20:e00133, 2019.
- [32] Sasin Pringpong, Sakkakom Maneenop, and Anutchanat Jaroenjitrkam. Geopolitical risk and firm value: Evidence from emerging markets. *The North American Journal of Economics and Finance*, 68:101951, 2023.
- [33] Donald B Percival and Peter Gutterp. Long-memory processes, the allan variance and wavelets. In *Wavelet analysis and its applications*, volume 4, pages 325–344. Elsevier, 1994.
- [34] Donald B Percival and Andrew T Walden. *Wavelet methods for time series analysis*, volume 4. Cambridge university press, 2000.
- [35] Shahriar Yousefi, Iona Weinreich, and Dominik Reinartz. Wavelet-based prediction of oil prices. *Chaos, Solitons & Fractals*, 25(2):265–275, 2005.
- [36] Keshab Shrestha and Kok Hui Tan. Real interest rate parity: long-run and short-run analysis using wavelets. *Review of Quantitative Finance and Accounting*, 25:139–157, 2005.
- [37] Patrick M Crowley. A guide to wavelets for economists. *Journal of Economic Surveys*, 21(2):207–267, 2007.
- [38] Junghwan Jin and Jinsoo Kim. Forecasting natural gas prices using wavelets, time series, and artificial neural networks. *PloS one*, 10(11):e0142064, 2015.
- [39] Bai-Ling Zhang, Richard Coggins, Marwan A Jabri, Dominik Dersch, and Barry Flower. Multiresolution forecasting for futures trading using wavelet decompositions. *IEEE Transactions on Neural Networks*, 12(4):765–775, 2001.
- [40] Bai-Ling Zhang and Zhao-Yang Dong. An adaptive neural-wavelet model for short term load forecasting. *Electric power systems research*, 59(2):121–129, 2001.
- [41] D Benaouda, Fionn Murtagh, J-L Starck, and Olivier Renaud. Wavelet-based nonlinear multiscale decomposition model for electricity load forecasting. *Neurocomputing*, 70(1-3):139–154, 2006.
- [42] Zhongfu Tan, Jinliang Zhang, Jianhui Wang, and Jun Xu. Day-ahead electricity price forecasting using wavelet transform combined with arima and garch models. *Applied energy*, 87(11):3606–3610, 2010.
- [43] Christian Dunis and Mark Williams. Modelling and trading the eur/usd exchange rate: Do neural network models perform better? *Derivatives use, trading and regulation*, 8(3):211–239, 2002.
- [44] Sangbae Kim and Francis In. The relationship between stock returns and inflation: new evidence from wavelet analysis. *Journal of empirical finance*, 12(3):435–444, 2005.
- [45] António Rua and Luis C Nunes. A wavelet-based assessment of market risk: The emerging markets case. *The Quarterly Review of Economics and Finance*, 52(1):84–92, 2012.
- [46] Kaijian He, Kin Keung Lai, and Jerome Yen. Ensemble forecasting of value at risk via multi resolution analysis based methodology in metals markets. *Expert Systems with Applications*, 39(4):4258–4267, 2012.
- [47] Antonios K Alexandridis and Mohammad S Hasan. Global financial crisis and multiscale systematic risk: Evidence from selected european stock markets. *International Journal of Finance & Economics*, 25(4):518–546, 2020.
- [48] Victor M Becerra, Roberto KH Galvão, and Magda Abou-Seada. Neural and wavelet network models for financial distress classification. *Data Mining and Knowledge Discovery*, 11:35–55, 2005.

- [49] Robert J Hodrick and Edward C Prescott. Postwar us business cycles: an empirical investigation. *Journal of Money, credit, and Banking*, pages 1–16, 1997.
- [50] Lawrence J Christiano and Terry J Fitzgerald. The band pass filter. *international economic review*, 44(2):435–465, 2003.
- [51] Rob J Hyndman and George Athanasopoulos. *Forecasting: principles and practice*. OTexts, 2018.
- [52] David A Pierce and Larry D Haugh. Causality in temporal systems: Characterization and a survey. *Journal of econometrics*, 5(3):265–293, 1977.
- [53] Aslak Grinsted, John C Moore, and Svetlana Jevrejeva. Application of the cross wavelet transform and wavelet coherence to geophysical time series. *Nonlinear processes in geophysics*, 11(5/6):561–566, 2004.
- [54] Donald B Percival and Harold O Mofjeld. Analysis of subtidal coastal sea level fluctuations using wavelets. *Journal of the American Statistical Association*, 92(439):868–880, 1997.
- [55] David E Rumelhart, Geoffrey E Hinton, and Ronald J Williams. Learning representations by back-propagating errors. *nature*, 323(6088):533–536, 1986.
- [56] Alex Aussem and Fionn Murtagh. Combining neural network forecasts on wavelet-transformed time series. *Connection Science*, 9(1):113–122, 1997.
- [57] Madhurima Panja, Tanujit Chakraborty, Uttam Kumar, and Nan Liu. Epicasting: An ensemble wavelet neural network for forecasting epidemics. *Neural Networks*, 2023.
- [58] Skander Soltani. On the use of the wavelet decomposition for time series prediction. *Neurocomputing*, 48(1-4):267–277, 2002.
- [59] Mina Aminghafari and Jean-Michel Poggi. Forecasting time series using wavelets. *International Journal of Wavelets, Multiresolution and Information Processing*, 5(05):709–724, 2007.
- [60] George EP Box and David A Pierce. Distribution of residual autocorrelations in autoregressive-integrated moving average time series models. *Journal of the American statistical Association*, 65(332):1509–1526, 1970.
- [61] David Salinas, Valentin Flunkert, Jan Gasthaus, and Tim Januschowski. Deepar: Probabilistic forecasting with autoregressive recurrent networks. *International Journal of Forecasting*, 36(3):1181–1191, 2020.
- [62] M Hashem Pesaran, Yongcheol Shin, et al. *An autoregressive distributed lag modelling approach to cointegration analysis*, volume 9514. Department of Applied Economics, University of Cambridge Cambridge, UK, 1995.
- [63] Tianqi Chen and Carlos Guestrin. Xgboost: A scalable tree boosting system. In *Proceedings of the 22nd acm sigkdd international conference on knowledge discovery and data mining*, pages 785–794, 2016.
- [64] Julian Faraway and Chris Chatfield. Time series forecasting with neural networks: a comparative study using the air line data. *Journal of the Royal Statistical Society Series C: Applied Statistics*, 47(2):231–250, 1998.
- [65] Alex J Koning, Philip Hans Franses, Michele Hibon, and Herman O Stekler. The m3 competition: Statistical tests of the results. *International Journal of Forecasting*, 21(3):397–409, 2005.
- [66] Vladimir Vovk, Alexander Gammernan, and Glenn Shafer. *Algorithmic learning in a random world*, volume 29. Springer, 2005.
- [67] Andrew T Walden. Wavelet analysis of discrete time series. In *European Congress of Mathematics*, pages 627–641. Springer, 2001.
- [68] Peifeng Li, Pei Hua, Dongwei Gui, Jie Niu, Peng Pei, Jin Zhang, and Peter Krebs. A comparative analysis of artificial neural networks and wavelet hybrid approaches to long-term toxic heavy metal prediction. *Scientific reports*, 10(1):1–15, 2020.
- [69] Yu Yang and Jun Wang. Forecasting wavelet neural hybrid network with financial ensemble empirical mode decomposition and mcid evaluation. *Expert Systems with Applications*, 166:114097, 2021.
- [70] Li Zhu, Yanxin Wang, and Qibin Fan. Modwt-arma model for time series prediction. *Applied Mathematical Modelling*, 38(5-6):1859–1865, 2014.

- [71] J-C Pesquet, Hamid Krim, and Hervé Carfantan. Time-invariant orthonormal wavelet representations. *IEEE transactions on signal processing*, 44(8):1964–1970, 1996.
- [72] Peter CB Phillips and Zhentao Shi. Boosting the hodrick-prescott filter. 2019.
- [73] Ramazan Gençay, Faruk Selçuk, and Brandon J Whitcher. *An introduction to wavelets and other filtering methods in finance and economics*. Elsevier, 2001.
- [74] Morten O Ravn and Harald Uhlig. On adjusting the hodrick-prescott filter for the frequency of observations. *Review of economics and statistics*, 84(2):371–376, 2002.

7 Appendix:

7.1 Discrete Wavelet Transformation:

The FEWNet framework leverages a form of discrete wavelet transformation (DWT) to first denoise the CPI inflation series for the BRIC countries followed by modeling of the resulting components with the auxiliary information (trend and cycle generated through HP and CF filters) using ARNNx [64] in an ensemble setup. In particular, we focus on the ‘maximal overlapping’ version of the DWT popularly known as MODWT. In the literature, the DWT framework has been widely used in various applications for compressing digital images, smoothing signals [34, 67], material science [68], atmosphere [54], energy [69], economics, and geophysics [70] among many others. We begin with a brief description of the DWT approach that forms the mathematical basis of the MODWT to be used in our proposed FEWNet framework.

The DWT approach defines a class of orthogonal wavelet transformation [33]. Let $\{h_l; l = 0, 1, \dots, L - 1\}$ denote a finite length discrete high-pass (wavelet) filter such that it satisfies the unit energy assumptions and it sums up to zero i.e.,

$$\sum_{l=0}^{L-1} h_l^2 = 1 \text{ and } \sum_{l=0}^{L-1} h_l = 0. \quad (7)$$

Furthermore, the wavelet filters are also restricted to be orthogonal to even shifts. Thus mathematically we can denote this as

$$\sum_{l=0}^{L-1} h_l h_{l+2\tilde{n}} = 0 \text{ for any non zero integer } \tilde{n}. \quad (8)$$

Alongside the high-pass filter, having a low-pass (scaling) filter $\{g_l; l = 0, 1, \dots, L - 1\}$ is also crucial for decomposing an observed time series into high-frequency oscillations and low-frequency details. These scaling filters also satisfy the unit energy assumptions and are orthogonal to even shifts (as in Eqs. (7), (8)). Furthermore, for all the wavelet filters, the low-pass filter coefficients are determined by the ‘quadrature mirror’ relationship i.e., $g_l = (-1)^{l+1} h_{L-1-l}$ or $h_l = (-1)^l g_{L-1-l}$; $l = 0, 1, \dots, L - 1$.

For the construction of DWT coefficients from a given series the use of the ‘pyramid algorithm’ is prevalent [33, 34]. Suppose we denote the economic time series to be transformed as $Y = \{Y_t, t = 1, 2, \dots, \mathcal{N}\}$ of length ($\mathcal{N} = 2^{\mathcal{K}}$). In the pyramid algorithm, given the series Y , the wavelet filters h_l , and the scaling filters g_l , the first iteration performs a down-sampling operation and convolutes the data vector with each of the filters to obtain the resulting wavelet and scaling coefficient. In the subsequent step, similar down-sampling and convolution take place on the scaling coefficients of the previous step. Following this procedure iteratively the \tilde{k}^{th} stage output of the pyramid algorithm can be expressed as

$$\varpi_{\tilde{k},t} = \sum_{l=0}^{L_{\tilde{k}}-1} h_{\tilde{k},l} Y_{2^{\tilde{k}}(t+1)-l \bmod \mathcal{N}} \text{ and } v_{\tilde{k},t} = \sum_{l=0}^{L_{\tilde{k}}-1} g_{\tilde{k},l} Y_{2^{\tilde{k}}(t+1)-l \bmod \mathcal{N}}, \quad (9)$$

where $\varpi_{\tilde{k},t}$ and $v_{\tilde{k},t}$ are the \tilde{k}^{th} ($\tilde{k} = 1, 2, \dots, \mathcal{K}$) level wavelet and scaling coefficients respectively. This procedure can be repeated for upto $\log_2(\mathcal{N})$ times. Thus using the DWT on the given time series, we can represent the discrete wavelet coefficients in matrix notation as

$$\varpi = \mathcal{W}Y, \quad (10)$$

where \mathcal{W} , an orthogonal matrix of order $\mathcal{N} \times \mathcal{N}$, comprises of wavelet and scaling filters arranged in a row-by-row basis. The wavelet coefficients ϖ can be arranged into $\mathcal{K} + 1$ vectors as $\varpi = [\varpi_1, \varpi_2, \dots, \varpi_{\mathcal{K}}, v_{\mathcal{K}}]^T$ with each of

$\tilde{\omega}_{\tilde{k}}$, ($\tilde{k} = 1, 2, \dots, \mathcal{K}$), a vector of length $\mathcal{N}/2^{\tilde{k}}$, consists of the wavelet coefficients associated with changes on a scale of length $2^{\tilde{k}-1}$ and the vector $v_{\mathcal{K}}$ of length $\mathcal{N}/2^{\mathcal{K}}$ is associated with averages on a scale of length $2^{\mathcal{K}-1}$.

Although the DWT is a useful mathematical tool for decomposing discrete time series into simpler parts using high-pass and low-pass filters, it suffers from certain serious limitations. To begin with, the DWT approach down-samples the signal at each iteration and it can be repeated for a maximum of $\log_2(\mathcal{N})$ thus restricting the size of the signal to be an exact power of 2. Moreover, the wavelet and scaling coefficients generated from a DWT convoluted signal do not scale and are not shift invariant. This restricts the universal application of the DWT algorithm for arbitrary time series. To overcome these deficiencies of the DWT framework a modified maximal overlapping version of DWT was proposed [33, 34, 67].

7.1.1 MODWT approach

The maximal overlapping discrete wavelet transform (MODWT) is an improved, non-subsampled version of the DWT framework. The MODWT overcomes the limitations of the DWT approach and is invariant to circular shifts. This non-decimated wavelet transform is suitable for handling the non-stationary behavior of a discrete-time process and is highly redundant. Moreover, the variance estimator pertaining to the MODWT process is asymptotically more efficient than that of the DWT [33]. Thus in our study, we utilize the transition and time-invariant [71] MODWT transformation for denoising the CPI inflation series. The mathematical formulation of the MODWT algorithm can be extended from the DWT approach and is described below.

For the MODWT algorithm, we define the rescaled version of filters as $\tilde{h}_l = h_l/2^l$ and $\tilde{g}_l = g_l/2^l$ and employ the pyramid algorithm with the time series Y , wavelet filter \tilde{h}_l , and scaling filter \tilde{g}_l . Similar to the DWT approach in the non-decimated MODWT framework the pyramid algorithm convolutes the data with the re-normalized filters and generates the resulting coefficients of length \mathcal{N} as

$$\tilde{\omega}_{\tilde{k},t} = \sum_{l=0}^{L_{\tilde{k}}-1} \tilde{h}_{\tilde{k},l} Y_{(t+1)-l \bmod \mathcal{N}} \quad \text{and} \quad \tilde{v}_{\tilde{k},t} = \sum_{l=0}^{L_{\tilde{k}}-1} \tilde{g}_{\tilde{k},l} Y_{(t+1)-l \bmod \mathcal{N}},$$

where $L_{\tilde{k}} = (2^{\tilde{k}} - 1)(L - 1) + 1$. The wavelet ($\tilde{\omega}_{\tilde{k},t}$) and scaling ($\tilde{v}_{\tilde{k},t}$) coefficients obtained by decomposing the data vector Y using the MODWT approach into \mathcal{K} levels can be formulated as

$$\tilde{\omega} = \tilde{\mathcal{W}}Y \tag{11}$$

where the orthonormal matrix $\tilde{\mathcal{W}} = [\tilde{\mathcal{W}}_1, \tilde{\mathcal{W}}_2, \dots, \tilde{\mathcal{W}}_{\mathcal{K}}, \tilde{\mathcal{V}}_{\mathcal{K}}]^T$ is made up of $\mathcal{K} + 1$ submatrices of size $\mathcal{N} \times \mathcal{N}$ with $\tilde{\mathcal{W}}_{\tilde{k}}$, ($\tilde{k} = 1, 2, \dots, \mathcal{K}$) and $\tilde{\mathcal{V}}_{\mathcal{K}}$ denoting circularly shifted wavelet and scaling filters respectively. Furthermore, the wavelet and scaling coefficients can be arranged in $\mathcal{K} + 1$ vectors as $\tilde{\omega} = [\tilde{\omega}_1, \tilde{\omega}_2, \dots, \tilde{\omega}_{\mathcal{K}}, \tilde{v}_{\mathcal{K}}]^T$ in a similar manner as in Eq. (10) of DWT approach.

Following the MODWT decomposition, an additive multi-resolution analysis (MRA) of the observed time series Y can be formulated as

$$Y_t = \sum_{\tilde{k}=1}^{\mathcal{K}} d_{\tilde{k},t},$$

where $d_{\tilde{k},t}$, $t = 1, 2, \dots, \mathcal{N}$ is the t^{th} element of $d_{\tilde{k}} = \tilde{\mathcal{W}}_{\tilde{k}} \tilde{\omega}_{\tilde{k}}$, ($\tilde{k} = 1, 2, \dots, \mathcal{K}$). Thus, the time series Y can be expressed as a linear combination of the high-frequency and low-frequency coefficients as

$$Y_t = S_{\mathcal{K},t} + \sum_{\tilde{k}=1}^{\mathcal{K}} \delta_{\tilde{k},t},$$

where $S_{\mathcal{K},t} = \sum_{j=\tilde{k}+1}^{\mathcal{K}+1} d_{j,t}$ is the \mathcal{K}^{th} level smooth coefficient and $\delta_{\tilde{k},t} = \sum_{j=1}^{\tilde{k}} d_{j,t}$ is the \tilde{k}^{th} level details associated with the MODWT-based MRA decomposition. A salient feature of this scale-based additive transformation is that the wavelet and scaling coefficients of the series are associated with the zero-phase filters. Hence, they are of the same size as the original series and are perfectly aligned with it. A more detailed structural overview of the MODWT process can be found in [54].

7.2 Economic filters - Hodrick-Prescott and Christiano-Fitzgerald filters:

The Hodrick-Prescott filter is a popular econometric method that has found profound applications in extracting the business cycle components and as a detrending method for financial time series [49]. The method is named after its proponents: - Robert J. Hodrick and Edward C. Prescott. This nonparametric method is widely adopted by economists in central banks, international economic agencies, industry, and in government sector [72]. There is a wide array of time series filters commonly used in macroeconomic and financial research and analysis to decompose the overall time series into trend, cycle, and irregular components [73]. Among them, the HP filter has been in vogue among researchers for extracting trend and cycle components from the time series. One key aspect of the HP filter is that it is quite effective and can be applied to non-stationary time series and therefore makes an excellent choice for decomposing CPI inflation, EPU, and GPRC series in this exercise.

For any time series data ($Y_t : t = 1, \dots, n$), the HP filter decomposes the series into a trend (τ_t), and a cyclical component (C_t), by solving the following minimization problem with respect to τ_t :

$$\hat{\tau}_t^{HP} = \underset{\tau_t}{\operatorname{argmin}} \left\{ \sum_{t=1}^n (Y_t - \tau_t)^2 + \theta \sum_{t=2}^n (\Delta^2 \tau_t)^2 \right\} \text{ and } \hat{C}_t^{HP} = Y_t - \hat{\tau}_t^{HP}$$

where $\Delta \tau_t = \tau_t - \tau_{t-1}$, $\Delta^2 \tau_t = \Delta \tau_t - \Delta \tau_{t-1} = \tau_t - 2\tau_{t-1} + \tau_{t-2}$, and $\theta \geq 0$ is a tunable parameter that controls the extent of penalty for fluctuations in the second differences of Y_t or in other words, it controls for the volatility in the trend component. The greater the value of θ , the more stable the trend component is. The choice of θ is determined by the user. Quite interestingly, the residual term or deviation from the trend term: ($Y_t - \hat{\tau}_t^{HP}$) is defined as the business cycle components. Thus, the HP filter can be considered as a ‘‘highpass filter’’, removing the trend components and returning high-frequency components in \hat{C}_t^{HP} . Let’s assume that a time series be expressed as: $Y_t = \tau_t + C_t$ (where C_t incorporates the effect of any irregular term). If C_t and the 2nd difference of τ_t are normally and independently distributed, the HP filter would be an ‘‘optimal filter’’ and θ is given as the ratio of the two variances: $\frac{\sigma_C^2}{\sigma_{\Delta^2 \tau}^2}$, where Δ^2 is the 2nd difference operator as defined earlier.

One very interesting property of θ is that, in the limiting case, when $\theta \rightarrow \infty$, the trend component becomes a linear time trend. In common practice, $\theta = 1600$ is used, as prescribed by [49], when HP filter is applied to quarterly US economic data. For other frequencies like annual or monthly data, $\theta = 6.25$ and $\theta = 129,600$ are used as default values [74]. The cyclical or residual component derived from the HP filters have the following frequency response function [73]:

$$\mathcal{H}(f, \theta) = \frac{4\theta[1 - \cos(2\pi f)]^2}{1 + 4\theta[1 - \cos(2\pi f)]^2}$$

and the trend component of the HP filter is given by:

$$\tau_t = \frac{\phi_1 \phi_2}{\theta} \left[\sum_{j=0}^{\infty} (A_1 \phi_1^j + A_2 \phi_2^j) Y_{t-j} + \sum_{j=0}^{\infty} (A_1 \phi_1^j + A_2 \phi_2^j) Y_{t+j} \right],$$

where ϕ_1 and ϕ_2 are the complex conjugates and depends on the value of θ and A_1 and A_2 are the functions of ϕ_1 and ϕ_2 . By this analysis, it can be argued that the trend component, extracted using the HP filter is a centered moving average term.

On the other hand, the Christiano-Fitzgerald (CF) (often regarded as a random walk filter) filter is a band pass filter that was primarily constructed using very similar principles as Baxter and King (BK) filter [50]. CF filter has demonstrated better performance compared to the BK filter in the case of real-time applications. CF filter can be calculated as:

$$C_t = \varphi_0 Y_t + \varphi_1 Y_{t+1} + \dots + \varphi_{T-1-t} Y_{T-1} + \tilde{\varphi}_{T-t} Y_T + \varphi_1 Y_{t-1} + \dots + \varphi_{t-2} Y_2 + \tilde{\varphi}_{t-1} Y_1$$

Where $\varphi_j = \frac{\sin(jb) - \sin(ja)}{\pi j}$, $j \geq 1$, and $\varphi_0 = \frac{b-a}{\pi}$, $a = \frac{2\pi}{p_u}$, $b = \frac{2\pi}{p_l}$ and $\tilde{\varphi}_k = -\frac{1}{2}\varphi_0 - \sum_{j=1}^{k-1} \varphi_j$. The parameters, p_u and p_l represent the break-off point of cycle length in the month. Any cycle value between p_u and p_l is preserved in the cyclical term C_t . CF filter aims to formulate the de-trending and smoothing problem in the frequency domain. CF filter approximates the ideal infinite bandpass filter like the BK filter. One key advantage of CF filters is that the random walk filter can exploit the complete series for the calculation of each filtered point. CF filters can converge well to optimal filters in the long run. This property speaks for the effectiveness of the CF filter as compared to the BK filter in the context of extracting meaningful features (cyclical components) from a specific time series.

In this analysis, the HP filter has been explored to extract the trend component for CPI inflation, EPU, and GPRC series Whereas, the CF filter is used to extract the cyclical terms from all the 3-time series (CPI inflation, EPU, and GPRC) and post that these derived features are used in the downstream FEWNet algorithm to generate the long-term forecasts for the CPI inflation series.

7.3 Conformal Prediction for semi-long term

Figure 6 depicts the uncertainty quantification of the FEWNet framework for the 12-month ahead forecast horizon. The conformal prediction intervals demonstrated in the figure are of varied widths across countries. In the case of 12-month forecasts for Brazil, the width of the interval averages around 5.06, while for Russia, it hovers around 2.3, for India, it averages 3.7, and the width value for China is around 6.03, the maximum among all the countries. This indicates a higher degree of prediction uncertainty for China as compared to the other countries.

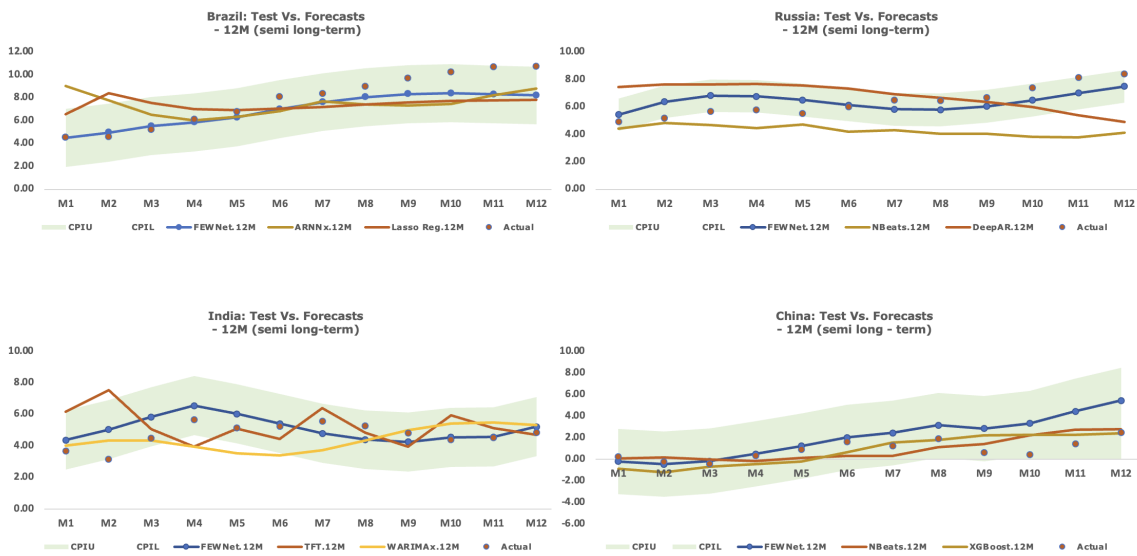


Figure 6: The plot shows the ground truth CPI inflation data (red dots), forecast generated by the best (yellow) and second-best (orange) baseline models for each country, conformal prediction interval (green shaded), and forecast (blue) generated by the FEWNet model for the semi-long term forecast horizon in BRIC Countries